Tetralactam-based Anion Transporters

Alexander M. Gilchrist,[1] Daniel A. McNaughton,[2] Mohamed Fares,[1,3] Xin Wu,[4] Bryson A. Hawkins,[3] Stephen J. Butler,[5] David E. Hibbs,[2] and Philip A. Gale[2,6,*]

[1]School of Chemistry, The University of Sydney, Sydney, New South Wales, 2006, Australia.
[2]School of Mathematical and Physical Sciences, University of Technology Sydney, Sydney, New South Wales, 2007, Australia.
[3]School of Pharmacy, The University of Sydney, Sydney, New South Wales, 2006, Australia.
[4]School of Pharmaceutical Sciences, Xiamen University, Xiamen, Fujian, 361102, China.
[5]Department of Chemistry, Loughborough University, Epinal Way, Loughborough, Leicestershire, LE11 3TU, U.K.
[6]Lead contact.
*Correspondence: philip.gale@uts.edu.au

SUMMARY

Synthetic anion transporters provide a promising avenue to treat diseases like cystic fibrosis and cancer. Anion binding site preorganisation is one aspect of transporter design which can be manipulated to enhance binding. Macrocycles possess preorganised binding cavities, enabling more stable, selective, and efficient anion binding and transport. In this study, we build on a macrocyclic tetralactam scaffold by preparing a series of fluorinated and non-fluorinated tetralactam anion transporters. Anion binding and transport assays were used to analyse the substituent effects on scaffold lipophilicity, selectivity, solubility, binding strength, and transport rates. The series was analysed for the ability to bind and transport Cl^- and F^- anions across lipid bilayers. Some highly fluorinated tetralactams display extremely high levels of Cl^- and F^- transport activity, showing record activities in HPTS assays and a Eu(III) probe-based F^- transport assay.

INTRODUCTION

Anion transport is an essential cellular function facilitated by membrane-bound ion channels.[1] Diseases in which genetic problems affect the structure of ion channels and hence reduce or stop the flow of anions through the membrane are known as channelopathies and include cystic fibrosis (CF).[2,3] In CF, reduction in the flow of chloride and bicarbonate through epithelial cell membranes in the lungs limits water osmosis, which leads to the formation of sticky mucus and continual lung infections, reducing the life expectancy of CF patients.[4,5] It has been proposed that small molecules which can facilitate anion transport through cell membranes, known as a 'channel replacement therapy', may ameliorate the symptoms of CF and other channelopathies by replacing the function of faulty channels.[6]

Small molecule anion transporters can dissipate pH gradients across lipid bilayer membranes. The natural product prodigiosin is one such transporter capable of depolarising acidic compartments within cancer cells. Prodigiosin functions as a H^+/Cl^- co-transporter, protonating, binding chloride and then diffusing across the lipid bilayer.[7] However, other synthetic small molecule transporters can diffuse pH gradients either by functioning as weak acid protonophores or by transporting deprotonated fatty acid carboxylate head groups, which, when reprotonated, can diffuse back across the membrane.[8-10] Shin and co-workers have shown that transporters that facilitate chloride transport across lipid bilayer membranes can trigger apoptosis in cancer cells, whilst compounds capable of transporting HCl can increase the pH in lysosomes in cells, interfering with autophagy.[11,12] Consequently, significant efforts have been directed towards developing compounds that transport chloride without dissipating pH gradients, as well as compounds capable of facilitating efficient HCl transport.[7,8]

Fluorination of anionophore scaffolds has been used to adjust their overall anion binding strength and lipophilicity, resulting in more effective transmembrane anion transporters across many classes of compounds, including tripodal and tetrapodal thioureas and *o*-phenylenediamine-based bis ureas.[13-17] Macrocycles offer the ability to tune and customise the exterior of the scaffold and, ultimately, the molecular properties of the overall structure without impeding the anion binding ability of the central cavity. Additionally, macrocyclic structures[18] offer greater encapsulation and binding site preorganisation, harbouring a more favourable and size-selective environment for anion binding, which may result in high transport efficiency and anti-Hofmeister selectivity.[19] The potent combination was demonstrated in previously reported Cl^- selective fluorinated tetraurea macrocycle, which achieved Cl^- binding constants $>10^5$ M^{-1} in >50% aqueous mixtures and could perform highly efficient H^+/Cl^- co-transport.[10,19] A recent study on a series of fluorinated macrocyclic bambus[6]urils demonstrated very efficient and selective Cl^-/HCO_3^- antiport across cell membranes.[20]

The increase in transport efficiency conveyed through scaffold fluorination also increases transporter lipophilicity. Both lipophilicity and solubility are important aspects of transporter design; anion transporters with an optimal lipophilic balance are capable of efficiently permeating and traversing the lipid bilayer. Very efficient anion transporters like the fluorinated tetraurea

macrocycle can be used at significantly lower concentrations, enabling lower amounts of a potentially more insoluble but highly active transporter to be used. Talukdar and co-workers reported on three benzimidazolyl hydrazone H^+/Cl^- co-transporters and, using a modified HPTS assay, achieved extremely high transport activities at low transporter loading, between 0.00017–0.000022 mol%.[21] In 2019, Smith and co-workers reported the synthesis and anion binding properties of macrocyclic tetralactams, including tetralactam **4a** (Figure 1), which formed stable complexes with anions like Cl^- and F^-.[22] However, the anion transport abilities of the tetralactam scaffold was not studied.

To explore the anion binding and transport abilities of the tetralactam macrocyclic scaffold, herein we report the design, synthesis and characterisation of a series of variably fluorinated tetralactams (Figure 1, compounds **1a**–**4c**). Certain members of this series were found to be amongst the most effective small molecule transmembrane chloride and fluoride transporters reported to date.

RESULTS AND DISCUSSION

Synthesis

A two-step synthetic method was used to prepare the tetralactam series (**1a**–**4c**, Scheme 1, a). An additional step was required to produce the 5-(trifluoromethyl)isophthalic acid starting material from the 3-methyl-5-(trifluoromethyl)benzoic acid precursor through $KMnO_4$ oxidation in H_2O (100 °C) before treatment with HCl (1 M) over ice to yield the desired intermediate.[23] A previously reported substitution reaction was then used to produce the isophthaloyl chloride intermediates from the isophthalic acid starting materials in CH_2Cl_2, with two drops of DMF added as a catalyst with oxalyl chloride.[24]

The isophthaloyl chloride intermediates were used immediately without workup.[22,24] Residual oxalyl chloride was removed, and the flask was charged with dry CH_2Cl_2 and anhydrous tetrabutylammonium chloride (TBACl), which acted as a templating agent. The appropriate diamine was dissolved in dry CH_2Cl_2 and added dropwise to the reaction mixture over 10 min. As the macrocyclisation reaction occurred, partial precipitation of the product and side products occurred. The reaction was stopped at 10 min with the addition of either CH_3OH or by removal of the reaction solvent under reduced pressure. Short reaction times were employed to yield the kinetic [2+2] macrocycles preferentially over larger thermodynamic side products.[22,25] A series of solvent washes and triturations were performed to isolate the desired products before anion exchange was performed by stirring the crude products with KPF_6 in dry CH_3CN. The bound Cl^- anion was exchanged with the weakly coordinating PF_6^- anion, which was removed using excess H_2O to provide the pure tetralactams in yields ranging from <1% to 39% (Scheme 1, a). Despite the low yields of macrocyclization in the current work, we anticipate future improvement of the syntheses by using the dynamic covalent approach developed by Mastalerz and coworkers.[26]

Additionally, two previously reported acyclic compounds, **5** and **6**, were synthesised, which are structurally related to tetralactam **2a** (Scheme 1, b and c). Isophthalamide **5** was synthesised according to a modified method by Ishikawa *et al.* (Scheme 1, b).[27] The isophthaloyl chloride intermediate was prepared and then dissolved in dry CH_2Cl_2. Aniline was then added dropwise to the reaction mixture, producing a precipitate. The precipitate was filtered and washed with CH_2Cl_2 and *n*-hexane, then resuspended in $CHCl_3$:H_2O (1:1, *v/v*) with HCl (1 M). The desired product was then collected in the organic phase, dried over $MgSO_4$, and evaporated to isolate isophthalamide **5** in a 51% yield. Benzamide **6** was synthesised following the previously reported method by Costa *et al.*, where the *o*-phenylenediamine was first dissolved in dry CH_2Cl_2 before the dropwise addition of 3-fluorobenzoyl chloride.[28] The precipitate was collected and washed with CH_2Cl_2 and H_2O to isolate **6** in a 33% yield. For further synthetic methods, see the experimental procedures section, or for information regarding compound characterisation and associated spectra (Figure S1–S55), see the electronic supplementary information (ESI).

Crystallography

To gain further insights into and elucidate the structures of the tetralactam series, attempts were made to grow diffraction-quality single crystals of each compound using various techniques and system conditions. Due to the low yield of some compounds, receptor solutions made for NMR studies were collected and reused to grow crystals. Therefore, the majority of the successfully grown single crystals (**3c**, **2a·Cl⁻**, **2c·Cl⁻**, **3a·Cl⁻**, **4b·Cl⁻**, **2a·F⁻**, and **3a·F⁻**) were obtained from the slow diffusion of H_2O vapour into DMSO-d_6/H_2O (0.5%) solutions (1 mM), which contained a large excess of either TBACl or TBAF (Figure 2, a–c). The solid-state structures tabulated crystallographic information and CCDC deposition numbers for each of the obtained crystal structures can be found in the ESI (Figure S56–S63 and Table S1–S69). Tetralactam **1b·2Cl⁻** was dissolved in hot CH_2Cl_2 with an excess of TBACl. Once completely dissolved, the solution was allowed to cool to room temperature, and the mother liquor was separated from the resultant precipitate before being allowed to stand while single crystals grew.

The single crystal X-ray structure of receptor **2c·Cl⁻** complex (Figure 2, a) shows the rigid macrocyclic scaffold forming four N–H···Cl^- hydrogen bonding interactions with a Cl^- anion with bond lengths between 3.251–3.341 Å and two C–H···Cl^- hydrogen bonds with lengths between 3.411–3.427 Å. Rather than being bound within the cavity, the anion is situated just above the

plane, suggesting that the ionic radius of Cl^- is slightly too large for the macrocyclic cavity to accommodate. The solid-state structure of **3c** is reasonably planar (Figure 2, b). With no guest bound within the central cavity, two of the amide protons point up while the other two point down. Extended stacked structures were also observed in the solid state where the amide protons of one **3c** molecule participated in N–H···O intermolecular hydrogen bonding interactions with the urea oxygen atom of an adjacent receptor with interaction lengths between 2.846–3.138 Å. In contrast, the inclusion of the F^- atom directly within the binding cavity of **2a** resulted in a greater out-of-plane curvature of the **2a·F⁻** complex (Figure 2, c). All six directional hydrogen bond donors within the binding site are coordinated to the F^- anion with N–H···F^- interaction lengths between 2.827–3.013 Å and C–H···F^- hydrogen bonding interaction lengths between 2.953–2.961 Å.

The remaining structures have been included in the ESI. It was evident that the larger ionic radius of the Cl^- ion was not a good size match for the central tetralactam cavity. In all cases, the remaining host:guest Cl^- complexes (**2a·Cl⁻**, **3a·Cl⁻**, **4b·Cl⁻**) formed hydrogen bonding interactions above and below the plane of the cavity or resulted in the macrocyclic scaffold buckling to adjust the hydrogen bond donors into a more energetically favourable conformation (Figure S57, a, S60, and S63). In comparison, the other F^- complex, **3a·F⁻**, confirms that the atomic radius of the F^- anion is a perfect size match for the tetralactam cavities (Figure S61). Both F^- complexes contain F^- bound directly within the binding cavity. Similarly to the Cl^- complexes, the host macrocycles of the F^- complexes also buckled to reorient the hydrogen bond donors for guest binding interactions. While most of the Cl^- complexes obtained for the series show 1:1 guest binding, the solid-state structures of **1b·2Cl⁻** and **2a·2Cl⁻** also revealed the ability of 1:2 host:guest complex formation (Figure S56 and S57, b). In both instances, one anion was bound above the cavity by two amide protons and the other below the cavity by the other two amide protons. Notably, the same crystal that yielded the **2a·2Cl⁻** complex also produced the 1:1 complex (**2a·Cl⁻**), which exhibited all four direction amide protons forming hydrogen bonding interactions with the one Cl^- anion above the central cavity (Figure S57, a and b).

Anion Binding Studies

The tetralactam series (**1a**–**4c**) and the two acyclic compounds (**5** and **6**) were analysed for their ability to bind to Cl^- anions and F^- anions using ^{1}H-NMR binding studies. Host solutions in DMSO-d_6/H_2O (0.5%) of a constant receptor concentration (1 mM) were used to make the guest solutions, containing the titrant guest anion as the TBA^+ salt. During the binding studies, the guest solutions were titrated into the host solution, causing stepwise increases in the concentration of the anionic guest. The changing chemical shifts (ppm) of the resonances attributed to the protons of the host were tracked and inputted into the BindFit web applet to produce binding constants (K_a, Table 1).[29,30] For further synthetic methods, see the experimental procedures section or for information on the fitted experimental data, including errors and associated spectra, see Table S70, Figure S64–S79 in the ESI.

In all cases except for receptor **1b**, the shifts in the resonances attributed to the amide N–H proton and isophthalic C–H proton were fitted to 1:1 host:guest binding model, where the use of the 1:2 host:guest model was found to give a similar K_{11} value to that obtained by the 1:1 model suggesting that the binding of a second chloride ion is negligible within the chloride concentration range used in the titrations. Within the four different sub-series, the same pattern regarding the strength of binding affinities emerged, corresponding to the identity of the R_2 substituents. The receptors containing the naphthalene linkers (**1b**−**4b**) had the weakest binding affinities of the series, whilst slightly higher binding affinities were obtained for the unsubstituted phenylene receptors (**1a**−**4a**). Notably, compounds **1c**−**4c** containing 4,5-difluorophenylene moieties have binding constants ~2.7–4.5-fold larger than their respective phenylene and naphthalene-containing derivatives. A similar trend appeared for the R_1 substituents, generally following electron-withdrawing capability with a general order of NO_2 > CF_3 > F > *t*-Bu (**1** > **3** > **2** > **4**). The receptor with the highest anion binding constant of K_a = 2850 M^{-1} was receptor **1c**, which contained R_1 = NO_2 and R_2 = 4,5-difluorophenylene substituents (Table 1). The receptor with the weakest binding affinity was compound **4b** (R_1 = *t*-Bu and R_2 = naphthalene), which aligns with both trends. Limited solubility was observed for the tetralactams containing naphthalene moieties, which can be attributed to the greater tendency for the extended aromatic system to π-π stack and form aggregates in solution.

Acyclic compounds **5** and **6** were prepared to investigate the difference in the anion binding ability of the encapsulated and preorganised binding cavity of the macrocyclic tetralactam scaffold compared to its acyclic components. Compounds **5** and **6** correspond to the two acyclic halves of macrocycle **2a**. The Cl^- binding constants of both **5** and **6** were very low at K_a = 16 and 12 M^{-1}, respectively (Table 1). Comparing the low binding constants of **5** and **6** to the binding constant achieved by tetralactam **2a** of K_a = 545 M^{-1} highlights the benefits of binding site preorganisation (Table 1).

In a previous study by Smith and co-workers, it was shown that receptor **4a** could bind to F^- in pure DMSO-d_6 at 298 K with a K_a of 5.3 (± 0.8) × 10^4 M^{-1}.[22] The same study also noted that trace amounts of H_2O in the DMSO-d_6 produced HF_2^-, preventing accurate fitting.[22] Initial F^- binding studies (using TBAF) were performed with tetralactams **2a** and **3a** (1 mM) to discover if any difference would be observed in the more competitive DMSO-d_6/H_2O (0.5%) solvent system (Figure S68 and S72). Immediate

peak broadening was observed for the resonances attributed to the N–H and C–H proton peaks after adding the initial aliquot of the F^- guest. Further additions above 1 equiv. caused both the amide and isophthalic proton peaks to disappear. Increasing the concentration of F^- caused receptor deprotonation, which was indicated by discolouration of the titration solution during binding studies.

Anion Transport Studies

The Cl^-/NO_3^- Exchange Assay:

Tetralactams **1a**–**4c** were tested for their ability to transport anions across the lipid bilayer using the ion-sensitive electrode (ISE) based Cl^-/NO_3^- exchange assay. The assay was performed using synthetic large unilamellar vesicles (200 nm) formed from 1-palmitoyl-2-oleoyl-*sn*-glycerol-3-phosphocholine (POPC), prepared according to literature methods.[15,30] The vesicles contained an internal solution of NaCl (489 mM) suspended in an external solution of $NaNO_3$ (489 mM), with both solutions being buffered to pH 7.2 with a sodium phosphate salt buffer (5 mM) (Figure 3, a). Anion transport was initiated at t = 0 s by adding each tetralactam as DMSO solution, and the subsequent Cl^- efflux was recorded using the ISE (Figure 3, b). The 100% Cl^- efflux value required for data calibration was obtained by lysing the vesicles with detergent at t = 300 s and collecting a further 120 s of data before the collection was stopped at t = 420 s. For information regarding experimental methods, see the experimental procedures section, or for information on the fitted experimental data, including errors and associated spectra, see Table S71 and Figure S80–S90 in the ESI.

The generally low solubility of **1a**–**4c** in aqueous media caused difficulty in accurately assessing the transport activity under the required assay conditions and, in some cases, prevented the transport activity from being determined. Transporters **2a**, **2c**, **3a**, **3c**, and **4c** showed a reasonable level of transport activity at concentrations low enough that precipitation did not occur, which allowed accurate data to be acquired. The data was fit to the Hill equation (Equation 1) to obtain both the effective concentration of the transporter required to facilitate 50% of the total Cl^- efflux (EC_{50}) and the Hill coefficients (n, Table 2).

The calculated Hill coefficients of $n \approx 1$ showed that the tested tetralactams transported Cl^- in an approximate 1:1 host:guest stoichiometry, in line with both the 1:1 host:guest binding stoichiometry observed during binding studies (Table 1) and the 1:1 host:guest single crystal X-ray structures of **2c** and **3a** (Figure 2, a and c). The EC_{50} values demonstrated that the three transporters with the highest transport activity contain the 4,5-difluorophenylene-linker (**3c** > **2c** > **4c**). These findings agree with the observed ^{1}H-NMR binding trends, where the same compounds had the highest binding constants of their respective sub-series. Tetralactams **2a**, **3a**, and **4c** obtained EC_{50} values of 0.036, 0.096, and 0.015 mol%, respectively (Table 2), representing a moderate level of transport activity.

The two most active transporters of the series, **2c** and **3c**, had EC_{50} values of 0.0012 and 0.00043 mol%, respectively (Table 2). Previously, the most active synthetic transporter reported using this assay was a 3,5-bis(trifluoromethyl)phenyl substituted *o*-phenylenediamine-based transporter (EC_{50} = 0.0015 mol%).[16] The most active natural product tested using this assay was prodigiosin with an EC_{50} of 0.00064 mol%.[16] Comparing the EC_{50} values obtained for transporters **2c** and **3c** shows that they are the two most active synthetic Cl^- transporters reported using this assay. It is also of interest to compare **3c** with A.P Davis' powerful anion transporters based on cholapod, decalin and anthracene scaffolds using specific initial rate analysis.[31] The EC_{50} of compound **3c** (delivered externally) can be converted to a specific initial rate of 600 s^{-1} assuming first-order kinetics. This value is comparable to the deliverability-adjusted specific initial rates of the best cholapod (670 s^{-1}) and the best anthracene-bisurea (1700 s^{-1}). Such a comparison requires caution because different salt concentrations, lipid concentrations and lipid types were used. Based on the available data, however, it is likely that compound **3c** has at least similar Cl^- transport activities compared with the best cholapod and anthracene-based transporters, particularly noting that the Cl^-/NO_3^- exchange by **3c** is rate-limited by NO_3^- transport due to its small cavity being a poor fit for NO_3^- as demonstrated by our anion selectivity studies (vide infra).

The Cationophore Coupled Assay (Cl^- and F^-):

The tetralactam series was then tested using the cationophore coupled transport assay for their ability to perform electroneutral H^+/Cl^- (or OH^-/Cl^- antiport) co-transport and electrogenic Cl^- selective transport. Synthetic LUVs were produced in the same manner as the Cl^-/NO_3^- exchange assay, except the internal solution contained KCl (300 mM) and the external solution contained potassium gluconate (K-Gluc, 300 mM) with both solutions buffered to pH 7.2 using 4-(2-hydroxyethyl)-1-piperazineethanesulfonic acid (HEPES, 10 mM).[32] Transport was initiated when the transporters were added to the assay system as DMSO solutions and ended when the vesicles were lysed with detergent after 300 s. A baseline was obtained by adding the transporters to a system of untreated vesicles. When the transporters were tested for their ability to perform electrogenic transport, the vesicles were treated with the ionophore valinomycin (Vln, Figure 4, a), a strict K^+ uniporter. Alternatively, when the series was tested for the ability to transport Cl^- via an electroneutral H^+/Cl^- (or OH^-/Cl^-) co-transport pathway, the vesicles were treated with the ionophore monensin (Mon, Figure 4, b), an H^+/K^+ exchanger. For further assay details, see the experimental procedures section, or for more information on experimental data and associated spectra, see Figure S91–S115 in the ESI.

Due to the low aqueous solubility of the series, transporter concentrations of 0.05 mol% were required to obtain initial rate constants (k_{ini}, s^{-1}, Table 3), which were calculated using Equations 2–4. Even at a reduced concentration, the naphthalene-substituted transporters (**1**−**4b**) were relatively inactive, with **1b** and **4b** slowly precipitating out of solution. The electroneutral transport character (ENC) was calculated for each transporter. The ENC factors describe how well a compound can perform H^+/Cl^- co-transport over Cl^- uniport and are calculated by dividing the k_{ini} transport rate obtained from Mon-treated vesicles by the rate obtained from Vln-treated vesicles (Table 3). An ENC factor value > 1.0 is indicative of higher electroneutral transport activity.

The addition of the series to vesicles not treated with an additional cationophore resulted in negligible enhancements in Cl^- efflux. The k_{ini} rates were shown to increase concordantly with the Cl^- binding constants, most likely due to stronger binding affinities, which allowed for better anion recognition and binding in a competitive environment. As a result, each sub-series conformed to the k_{ini} rate order of 4,5-difluorophenylene- > phenylene- > naphthalene-linked tetralactams (**c** > **a** > **b**). Over the series, only the *t*-Bu-phenylene-linked transporter (**4a**) had an ENC factor below 1.3, indicating that the main transport pathway was via the electroneutral co-transport mechanism (Table 3). The k_{ini} rates obtained in untreated vesicles and vesicles treated with Vln were very similar for most of the series, indicating that the series does not operate via an electrogenic Cl^- pathway. Interestingly, the transporters containing higher degrees of fluorination displayed ENC factors of ≥ 3 (Table 3). The CF_3-substituted transporter containing the 4,5-difluorophenylene-linker (**3c**) was highly active and had to be tested at a 100-fold lower concentration of 0.0005 mol% compared to **3a** or **3b** (0.05 mol%). Even at a reduced concentration, tests still resulted in extremely high electroneutral transport activity with a k_{ini} = 0.25 mol% (Table 3).

Initial mechanistic investigations into electrogenic F^- transport were also performed due to the better size match with the tetralactam cavity for F^- compared to Cl^-. Due to the free diffusion of HF through the lipid bilayer when vesicles are treated with Mon, electroneutral H^+/F^- co-transport could not be investigated. The experiments required slight alterations to the conditions used in the regular cationophore coupled transport assay, which has been previously reported by our group.[33] An internal solution of KF was used instead of KCl, and a fluoride ISE was used. Generally, the phenylene-linked transporters facilitated low to moderate levels of electrogenic F^- uniport in the presence of Vln. Notably, the F-substituted naphthalene-linked transporter (**2c**) achieved the highest electrogenic F^- efflux of 57%; however, the other naphthalene-linked tetralactams performed very poorly. The 4,5-difluorophenylene-linked transporters also facilitated low to moderate levels of F^- efflux when tested with both Vln-treated and untreated vesicles, suggesting the ability to elicit unaided F^- transport and possibly very efficient H^+/F^- cotransport. Due to solubility and inactivity, each tetralactam was tested at different concentrations, preventing further comparisons by k_{ini} rates or EC_{50} values.

The HPTS Transport Selectivity Assay

The tetralactam series were then tested for their ability to facilitate H^+/Cl^- transport using the 8-hydroxypyrene-1,3,6-trisulfonic acid (HPTS) transport selectivity assay under three assay conditions.[34] Untreated vesicles were employed to analyse fatty acid flip-flop aided H^+/Cl^- co-transport mediated by transporters (Figure 5, a). The second condition utilises carbonyl cyanide-*m*-chlorophenylhydrazone (CCCP) treated vesicles, which acts as a weak acid protonophore, allowing the study of transporter-mediated Cl^- selective uniport (Figure 5, b). The final condition uses vesicles treated with bovine serum albumin (BSA). This protein is employed to sequester fatty acids from the lipid bilayer, enabling the study of transporter-mediated H^+/Cl^- co-transport in the absence of fatty acids (Figure 5, c). The vesicles contained the pH-sensitive probe HPTS (1 mM), NaCl (100 mM), and HEPES (10 mM) and were prepared following a previously reported method.[34] The LUVs were suspended in an external solution of NaCl (100 mM) and HEPES (10 mM), with both the internal and external solutions being buffered to pH 7. Transport was initiated when the transporters were added to the assay systems at varied concentrations as DMSO solutions, and the fractional fluorescence intensity was recorded. The data was then plotted (Figure 5, d) before being fitted to the Hill equation (Equation 1) to afford EC_{50} values and Hill coefficients (n). For further experimental methods, see the experimental procedures section, or for more information on experimental data and associated spectra, see Table S72–S73 and Figure S116–S151 in the ESI.

Fitting of the data to the Hill equation (Equation 1) showed that the transport facilitated by **1a**–**4c** was again in a 1:1 host:guest stoichiometry, indicated by Hill coefficients of $n \approx 1.0$ (Table 4). The stoichiometries are further supported by the 1:1 host:guest binding constants and the 1:1 host:guest Hill coefficients returned by the Cl^-/NO_3^- exchange assay. The exception to this general observation was **2a**, which yielded a Hill coefficient of $n \approx 2$, which is shown to be feasible in the solid-state structure of **1b**·**2Cl**$^-$ (Figure S56) at greater Cl^- concentrations (Table 4).

Under all three assay conditions, the 4,5-difluorophenylene-linked transporters showed the highest transport activity. Similar levels of transport activity were observed when the series was tested using CCCP-treated and untreated vesicles, indicating that negligible Cl^- uniport was occurring. Also, the transport activity significantly decreased in the absence of fatty acids when BSA-treated vesicles were used. The transport activity trends indicate that the primary mechanism of transport is the

electroneutral fatty acid flip-flop-aided H^+/Cl^- co-transport mechanism.[37] The defined tetralactam binding cavities means the series can also bind to the carboxylate head group of fatty acids. Interestingly, the CF_3-substituted transporters (**3a**–**3c**) produced lower EC_{50} values when fatty acids were sequestered from the lipid bilayers of the BSA-treated vesicles. This suggests that **3a**–**3c** are capable of efficient electroneutral H^+/Cl^- co-transport unaided by the fatty acid flip-flop mechanism. Alternatively, the slower transport aided by fatty acids could be the result of the complex formed between **3a**–**3c** and a fatty acid being too lipophilic, hindering membrane partitioning and slowing transport. The lipophilic balance achieved by the complexation of a fatty acid with **2a**–**2c** allows for very efficient unhindered fatty acid flip-flop.

The majority of the tetralactam series possessed extremely high transport activity, particularly the transporters with the highest degree of fluorination. Transporters **1c**−**4c** have exceptionally high transport activities and low EC_{50} values of 0.000078, 0.000028, 0.000044, and 0.00081 mol%, respectively (Table 4). The inversion in activity of **2c** > **3c** is possibly due to the ability of **2c** to competitively bind to a Cl^- anion with slightly weaker binding interactions compared to **3c**, allowing for easier guest capture and release as well as unhindered fatty acid flip-flop. Another possibility is that the decreased lipophilicity of **2c** compared to **3c** with CLogP values of 4.29 and 5.13, respectively (Table 4), enhances membrane permeability. The natural H^+/Cl^- co-transporter prodigiosin has also been previously studied using the HPTS transport assay, with an EC_{50} value of 0.000061 mol%.[10] The transport activities of **2c** and **3c** show a 2.2- and 1.4-fold increase in transport activity compared to prodigiosin, confirming the anionophores as the two most active H^+/Cl^- co-transporters explored using this assay.

The Adjusted HPTS Transport Selectivity Assay

Recently, Talukdar and co-workers reported on a series of benzimidazolyl hydrazone H^+/Cl^- co-transporters which were shown to be the most active synthetic transporters studied to date, with one compound returning an EC_{50} of 0.000022 mol%.[21] However, the transport properties of the series were investigated using an adjusted HPTS transport selectivity assay where a single excitation wavelength (450 nm) was used to excite the HPTS probe with an emission wavelength of 510 nm instead of a dual excitation wavelength. Other adjustments included the use of 100 nm L-α-phosphatidylcholine (EYPC) vesicles, buffered to pH 7.2, compared to the HPTS assay conditions above, which used 200 nm POPC vesicles buffered to pH 7.0. Due to these differences in experimental methods, anionophores **2c** and **3c** were tested using the conditions in the adjusted HPTS assay (Figure 6). For further information and fitted experimental spectra, see Figure S164–S165 in the ESI.

Compounds **2c** and **3c** both achieved greater activity under the conditions of the adjusted assay. The significant change in transport rate between the two studies can be attributed to the absolute rate of anion transport into a vesicle being proportionate to the vesicle surface area.[38] Previously, Davis and co-workers stated that only transporters capable of eliciting high transport activities would produce any significant difference in activity due to liposome size.[38] Tests performed using **2c** and **3c** indicated a 25% and 41% increase in transport activity, respectively (Table S74), compared to the previous HPTS transport selectivity study. Fitting the transport data to the Hill equation (Equation 1) resulted in EC_{50} values of 0.0000070 mol% and 0.000018 mol% for **2c** and **3c**, respectively. Additionally, the Hill coefficients obtained for **2c** and **3c** were both $n \approx 1$. Tetralactam **2c** achieved a 3.1-fold enhancement in transport activity compared to the best benzimidazolyl hydrazone co-transporter, while **3c** produced a 1.2-fold increase in H^+/Cl^- co-transport activity. These comparisons demonstrate that **2c** and **3c** display the highest H^+/Cl^- co-transport activities among any natural or synthetic Cl^- anionophores tested under the HPTS assay.

The HPTS 'Anion Gradient' Transport Selectivity Assay

The tetralactam series were also investigated for their preference to transport a range of anions as NaX salts (100 mM, X = Cl^-, Br^-, NO_3^-, I^-, and ClO_4^-) using the previously reported HPTS anion gradient transport selectivity assay.[39] Vesicles containing Cl^- were made the same way as the regular HPTS assay; however, the vesicles were suspended in different external solutions containing the anion of interest (Figure 7, a). Transport was initiated when the **1a**–**4c** were added as DMSO solutions where $Cl^- > X^-$ transport causes the basification of the internal solution, resulting in a positive ΔpH, while $X^- > Cl^-$ transport selectivity results in the acidification of the internal solution and a negative ΔpH (Figure 7, b). Equation 5–6 was then used to transform the fractional fluorescence intensity (I_f) data to the corresponding ΔpH value. Also, the greater the magnitude of the change of pH, the greater the preference of $X^- > Cl^-$ transport is for the transporter being studied. For further details on methods, see the experimental procedures section, or for information on experimental data and spectra, see Figure S152–S163 in the ESI.

The results show that there is a clear preference for the halide anions over the oxo-anions. The simple spherical geometry of the halide anions makes them a better geometrical fit for the tetralactam binding cavities than the complex geometries of the oxo-anions. Previously, a fluorinated tetraurea macrocycle containing a larger preorganised binding cavity consisting of eight convergent N–H hydrogen bond donors was studied using this assay, revealing the greatest transport selectivity for Cl^-.[19,39] In contrast, the suboptimal size-match between Cl^- and the tetralactam cavity prevents the selective transport of Cl^- over the other tested anions, leading to a clear selectivity preference for the larger halides instead.

The larger ionic radii of I^- (2.20 Å), Br^- (1.96 Å), and Cl^- (1.81 Å) prevents the anions from binding directly within the cavity, unlike F^- (1.33 Å).[40] The two hydrophobic oxo-anions NO_3^- (1.79 Å) and ClO_4^- (2.50 Å) had the lowest transport rate due to the poor geometrical fit hindering their binding to the rigid binding cavity.[40] However, further analysing the average halide selectivity sequence of $I^- > Br^- > Cl^-$ showed that along with a favourable geometry, transport selectivity increased as halide hydration enthalpies decreased, anion hydrophobicity increased, and ionic radii increased. Despite I^- binding to NH-based anion receptors generally observed to be weak in organic solvents, many NH-based anion transporters including the tetralactam series shows the highest selectivity for it over the other halides due to the lower free energy of solvation (ΔG_{hyd} = −280 kJ mol^{-1}) and higher hydrophobicity, enabling more efficient membrane partitioning.[40,41] Likewise, Br^- is more hydrophobic and has a weaker hydration energy (ΔG_{hyd} = −318 kJ mol^{-1}) than Cl^- (ΔG_{hyd} = −344 kJ mol^{-1}), accounting for the observed $Br^- > Cl^-$ transport selectivity.[40,41] Also aiding in the observed halide > oxo-anion selectivity are the enhanced binding interactions and greater stability afforded by the macrocyclic effect after the formation of the host:guest complexes.

The Eu(III) F^- Transport Assay

Having confirmed that **1a**–**1c** predominantly perform as highly active H^+/Cl^- co-transporters, it was envisaged that the tetralactams would also be capable of efficient electroneutral F^- co-transport. However, the ability of the series to perform electroneutral F^- co-transport could not be analysed using the standard suite of assays because the F^- cationophore coupled transport assay does not work in the presence of monensin. Previously, Butler synthesised a luminescent Eu(III) probe capable of detecting F^- in H_2O.[42] The probe is capable of F^- detection between 2–260 μM with no noticeable interference from a range of competing anions.[42] Using the same probe, an assay capable of direct F^-/Cl^- transport detection was developed by Butler, Valkenier, and co-workers.[43] The synthetic vesicles were made the same way as the regular HPTS assay and contained an internal solution of NaCl (225 mM), HEPES (0.5 mM), and the Eu(III) probe (50 μM) (Figure 8, a). The vesicles were then suspended in an external solution of NaCl (225 mM) and HEPES (0.5 mM), with both solutions being buffered to pH 7.0. A NaF base pulse with a final concentration of 3 mM was added to the system, and when no leakage was detected, the transporters were added at various concentrations as DMSO solutions (Figure 8, b). For further information on the fitted experimental data and associated spectra see Table S75 and Figure S166–S177 in the ESI.

Each experiment continued for a total of t = 750 s, with the vesicles being lysed with detergent after a total of t = 600 s. The experiments are longer than the HPTS transport assay due to the increased time required for transport equilibration to occur once the transporter has been added.[43] Hill fitting of the transport data at t = 600 s enabled both EC_{50} values and Hill coefficients (n) to be obtained for thorough analysis. Conforming to the previously established Cl^- transport activity trend, the highly fluorinated transporters **1c**, **2c**, **3c**, and **4c** displayed the highest activity in the series (Table 5).

The most active transporters with the lowest EC_{50} values were those substituted with the CF_3 groups, followed by the NO_2 > F > *t*-Bu-substituted transporters. Extremely high transport activity was achieved by **2c** with an EC_{50} of 0.0000048 mol% followed by **1c** with 0.0000088 mol%, **3c** at 0.000010 mol%, and finally **4c** with an EC_{50} value of 0.000098 mol% (Table 5). The enhanced F^- transport under this assay can partially be ascribed to the good size-fit complementarity of the smaller F^- anion inside the macrocyclic binding cavity. Valkenier, Butler, and co-workers tested the F^- transport properties of two cationic transporters previously reported by Gabbaï and co-workers, the best of which yielded an EC_{50} value of 0.000014 mol%.[43-45] Comparing the transport activities of **1a**–**4c** shows that the entire series is capable of highly efficient F^- transport. Further comparing the three most active tetralactams **1c**, **2c**, and **3c** with the best previously tested cationic F^- transporter displays 1.6-, 2.9-, and 1.4-fold enhancements in transport activity, placing them as the most active F^- transporters reported to date using this method.

Conclusions

In this work, we have synthesised and characterised a series of tetralactam macrocycle transporters based on the previously reported tetralactam **4a** and studied the Cl^- binding, Cl^- transport, F^- transport, and transport selectivity properties of each. Throughout the studies, the tetralactams containing fluorinated isophthalamide-substituents displayed the highest transport activities, but the aromatic linkers had the largest impact on anion transport. In all cases, the transporters containing the 4,5-difluorophenylene-linker linker displayed the strongest binding and highest transport activities. ^{1}H-NMR Cl^- binding studies demonstrated that the series was capable of moderate 1:1 host:guest binding, which was ideal for efficient anion recognition, capture, and release during transport. An important milestone was achieved when testing **2c** and **3c** using the ISE-based Cl^-/NO_3^- exchange transport assay, with results showing that they are the two most active transporters ever recorded using this method. Mechanistic transport studies revealed that the series primarily operates via an electroneutral H^+/Cl^- co-transport mechanism. Significantly, comparing the most potent transporters **2c** and **3c** to the best natural anionophore, prodigiosin, in the HPTS transport assay showed a 2.2- and 1.4-fold enhancement in H^+/Cl^- transport activity, respectively. The previously most active synthetic H^+/Cl^- transporter was analysed using an adjusted HPTS transport assay. This assay was recreated, and compounds **2c** and **3c** displayed a 3.1 and 1.2-fold enhancement in transport activity over this transporter, respectively. Thus, **2c** and **3c** are among the most active Cl^- transporters ever tested in vesicular assays. Finally, we analysed the F^-/Cl^- antiport ability of the entire series using a recently developed assay by Butler, Valkenier, and co-workers.[43] Hill analysis showed that

these transporters are also extremely active F^- transporters, with **1c**, **2c**, **3c**, and **4c** producing the highest F^- transport activities across the series.

EXPERIMENTAL PROCEDURES

Synthesis and Characterization of Intermediate Compounds

5-(Trifluoromethyl)isophthalic acid

The 5-(trifluoromethyl)isophthalic acid (**209**) was synthesised using a previously reported method.[23] 3-Methyl-5-(trifluoromethyl)benzoic acid (**206**, 1.00158 g, 1 equiv.) was suspended in H_2O (100 mL) and stirred at r.t. while $KMnO_4$ (3.10907 g, 4.01 equivs.) was added. The reaction mixture was then heated to reflux (100 °C, 373.15 K) over 16 h. The hot reaction mixture was then carefully filtered through a layer of celite (2–3 cm thick), and the filtrate was collected and allowed to cool. Once at r.t., the filtrate was acidified by adding conc. $HCl_{(aq)}$ (32%) with stirring to protonate the oxidised product. Slowly, a white solid precipitated from the solution, which was separated after stirring for a further 45 min, washed with H_2O (2×10 mL), and then dried *in vacuo* for 12 h. The solid was then redissolved in acetone and extruded through a PTFE 0.22 µM pore syringe filter to remove the insoluble brown impurities. The acetone filtrate was then evaporated under reduced pressure and dried in *vacuo* for 12 h to afford the white solid of **209** in a yield of 0.65330 g (57%).

^{1}H-NMR (300 MHz, DMSO-d_6): δ 13.82 (s, 2H), 8.68 (s, 1H), 8.38 (s, 2H). **^{13}C{^{1}H}-NMR** (75 MHz, DMSO-d_6): δ 165.2, 133.4, 132.8, 130.9–129.6 (m), 129.3, 125.1 (q). **^{19}F-NMR** (282 MHz, DMSO-d_6): δ −63.0.

The General synthetic procedure for the Isophthaloyl Chloride Intermediates

The isophthaloyl chloride intermediates were synthesised following a previously reported method.[24] The reaction flask was charged with the respective isophthalic acid starting material (1 equiv.), and the atmosphere was purged with $N_{2(g)}$ before CH_2Cl_2 (25 mL) was added and further degassed with $N_{2(g)}$ and DMF (2 drops, Cat.) was added. The reaction mixtures were allowed to stir for 10 min to ensure the homogeneity of the mixture before oxalyl chloride (2.2 equivs.) was added. The reaction was stirred for a further 10 min to allow the potential evolution of $HCl_{(g)}$ to be monitored, after which the reaction was heated to reflux (40 °C, 313.15 K). During each reaction, the isophthalic acids were observed to dissolve as the respective isophthaloyl chloride intermediates formed, which was indicated by a changed colour and the disappearance of the starting material suspended in solution.

Due to the instability and quick hydrolysis of the intermediates, the purity of each isophthaloyl chloride could not be checked. Since the isophthalic acids were partially insoluble under the reaction conditions, the reaction was deemed complete only once the reaction mixture was completely translucent with no noticeable starting material suspended in solution. Once the reactions were complete, an extra 1 h was added to the reaction time before the residual oxalyl chloride and CH_2Cl_2 was evaporated, collected in a cold trap, and the oxalyl chloride quenched. The reaction mixture was dried *in vacuo* for 3–12 h. The isolated isophthaloyl chloride intermediates were kept under $N_{2(g)}$ and often used immediately in the next step without further purification. An example has been provided below.

5-Nitroisophthaloyl dichloride

Using the general previously reported method above, the 5-nitroisophthalic acid starting material (0.44550 g) was suspended in CH_2Cl_2 (25 mL), and oxalyl chloride (0.87 mL, ~2.2 equivs.) was added before the reaction mixture was heated to reflux where the reaction proceeded quickly. The associated colour change for the nitro intermediate was a bright translucent yellow solution of the desired product, which was isolated as a bright yellow crystalline solid in a yield of 0.5234 g (100%).

Synthesis and Characterization of Compounds

4^5,10^5-Dinitro-2,6,8,12-tetraaza-1,7(1,2),4,10(1,3)-tetrabenzenacyclododecaphane-3,5,9,11-tetraone (Tetralactam 1a)

The reaction flask containing the 5-nitroisophthaloyl dichloride (0.52340 g) was evacuated and charged with dry $N_{2(g)}$. The pre-dried TBACl (2.93252 g, 5 equivs.) was pre-dissolved in CH_2Cl_2 (20 mL). The CH_2Cl_2:TBACl solution (10 mL) was added directly to the reaction flask and allowed to stir for 10 min. The *ortho*-phenylenediamine (0.25087 g, 1.1 equivs.) was pre-dissolved in the CH_2Cl_2:TBACl solution (10 mL) and then added to the reaction mixture over 2 min. After 10 min, the crude product was precipitated by adding CH_3OH (40 mL). The precipitate was separated and washed with H_2O (excess) and *n*-hexane (4×10 mL) to remove residual diamine. The crude was allowed to dry in the glass frit before being dissolved in a mixture of CH_2Cl_2 (40 °C, 15 mL) and TBACl (excess). The triturated mixture was placed in the freezer for 12 h, and the fine pale-yellow solid was separated and washed again with water (excess) and *n*-hexane (4×10 mL). The solid was collected, and anion exchange was then performed by suspending the solid in CH_3CN (150 mL), KPF_6 (10 equivs.) was added, and the mixture was stirred for 12 h. The fine light-yellow solid of **1a** was filtered and washed with H_2O (excess) before being dried *in vacuo*, with a final yield of 0.11261 g (9%).

^{1}H-NMR (600 MHz, DMSO-d_6): δ 10.52 (s, 4H), 9.09 (s, 2H), 8.94 (s, 4H), 7.94 (app. s, 4H), 7.39 (dd, *J* = 6.1, 3.6 Hz, 4H). **^{13}C{^{1}H}-NMR** (151 MHz, DMSO-d_6): δ 163.2, 148.0, 136.3, 133.1, 130.6, 126.2, 125.3, 125.1. **LR-MS** (ESI$^-$): [M+Cl]$^-$: 601.1 *m/z*. **HR-MS** (ESI$^-$) calculated for $C_{28}H_{17}N_6O_8$ [M−H]$^-$: 565.11164 *m/z*, found: 565.11134 *m/z*. **M.P.**: >350 °C (decomp.).

4^5,10^5-Dinitro-2,6,8,12-tetraaza-1,7(2,3)-dinaphthalena-4,10(1,3)-dibenzenacyclododecaphane-3,5,9,11-tetraone (Tetralactam 1b)
The reaction flask containing the 5-nitroisophthaloyl dichloride (0.58046 g) was evacuated and charged with dry $N_{2(g)}$. The pre-dried TBACl (3.25227 g, 5 equivs.) was pre-dissolved in CH_2Cl_2 (20 mL). The CH_2Cl_2:TBACl solution (10 mL) was added directly to the reaction flask and allowed to stir for 10 min. The 2,3-diaminonapthalene (0.4907 g, 1.1 equivs.) was pre-dissolved in the CH_2Cl_2:TBACl solution (10 mL) and then added to the reaction mixture over 2 min. After 10 min, the crude product was precipitated by adding CH_3OH (40 mL). The precipitate was separated and washed with H_2O (excess) and *n*-hexane (4×10 mL) to remove residual diamine. The crude was then triturated in boiling DMSO (10 mL), after which the solution was allowed to stand at r.t. while the Cl$^-$ complex slowly precipitated. Once at r.t., the solid was separated from the trituration mixture; it was washed again with water (excess) and *n*-hexane (4×10 mL). The solid was collected, and anion exchange was then performed by suspending the solid in CH_3CN (150 mL), KPF_6 (10 equivs.) was added, and the mixture was stirred for 12 h. The bright yellow solid was filtered and washed with H_2O (excess) before being dried *in vacuo*, with a final yield of 0.07751 g (6%).

^{1}H-NMR (800 MHz, DMSO-d_6): δ 10.78 (s, 4H), 10.19 (s, 2H), 8.84 (s, 4H), 8.56 (s, 4H), 7.94 (s, 4H), 7.52 (s, 4H). **^{13}C{^{1}H}-NMR** (201 MHz, DMSO-d_6): δ 163.7, 148.7, 136.0, 132.9, 131.1, 129.3, 127.8, 126.7, 126.3, 124.0. **LR-MS** (ESI$^-$): [M−H]$^-$ and [M+Cl]$^-$: 665.2 and 701.2 *m/z*, respectively. **HR-MS** (ESI$^-$) calculated for $C_{36}H_{21}N_6O_8$ [M−H]$^-$: 665.14264 *m/z*, found: 665.14300 *m/z*. **M.P.**: >309 °C (decomp.).

1^4,1^5,7^4,7^5-Tetrafluoro-4^5,10^5-dinitro-2,6,8,12-tetraaza-1,7(1,2),4,10(1,3)-tetrabenzenacyclododecaphane-3,5,9,11-tetraone (Tetralactam 1c)
The reaction flask containing the 5-nitroisophthaloyl dichloride (0.58889 g) was evacuated and charged with dry $N_{2(g)}$. The pre-dried TBACl (3.29947 g, 5 equivs.) was pre-dissolved in CH_2Cl_2 (20 mL). The CH_2Cl_2:TBACl solution (10 mL) was added directly to the reaction flask and allowed to stir for 10 min. The 1,2-diamino-4,5-difluorobenzene (0.37641 g, 1.1 equivs.) was also pre-dissolved in the CH_2Cl_2:TBACl solution (10 mL) and then added to the reaction mixture over 2 min. After 10 min, the crude product was precipitated by adding CH_3OH (40 mL). The precipitate was separated and washed with H_2O (excess) and *n*-hexane (4×10 mL) to remove residual diamine. The crude was then triturated in boiling DMSO (10 mL), after which the solution was allowed to stand at r.t. while the Cl$^-$ complex slowly precipitated. Once at r.t., the solid was separated from the trituration mixture; it was washed again with water (excess) and *n*-hexane (4×10 mL). The solid was collected, and anion exchange was then performed by suspending the solid in CH_3CN (150 mL), KPF_6 (10 equivs.) was added, and the mixture was stirred for 12 h. The off-white solid was filtered and washed with H_2O (excess) before being dried *in vacuo*, with a final yield of 0.25827 g (17%).

^{1}H-NMR (500 MHz, DMSO-d_6): δ 10.48 (s, 4H), 9.04 (s, 2H), 8.88 (s, 4H), 8.06 (t, *J* = 10.1 Hz, 4H). **^{13}C{^{1}H}-NMR** (201 MHz, DMSO-d_6): δ 163.1, 148.1, 146.0 (d, $^{1}J_{CF}$ = 245 Hz), 135.0, 132.7, 126.7, 126.1, 114.3. **^{19}F-NMR** (471 MHz, DMSO-d_6): δ -141.0. **LR-MS** (ESI$^-$): [M−H]$^-$ and [M+Cl]$^-$: 637.2 and 673.1 *m/z*, respectively. **HR-MS** (ESI$^-$) calculated for $C_{36}H_{21}N_6O_8$ [M−H]$^-$: 637.07365 *m/z*, found: 637.07373 *m/z*. **M.P.**: >400 °C (decomp.).

4^5,10^5-Difluoro-2,6,8,12-tetraaza-1,7(1,2),4,10(1,3)-tetrabenzenacyclododecaphane-3,5,9,11-tetraone (Tetralactam 2a)
The reaction flask containing the 5-fluoroisophthaloyl dichloride (0.30044 g) was evacuated and charged with dry $N_{2(g)}$. The pre-dried TBACl (1.88904 g, 5 equivs.) was pre-dissolved in CH_2Cl_2 (20 mL). The CH_2Cl_2:TBACl solution (10 mL) was added directly to the reaction flask and allowed to stir for 10 min. The *ortho*-phenylenediamine (0.16162 g, 1.1 equivs.) was pre-dissolved in the CH_2Cl_2:TBACl solution (10 mL) and then added to the reaction mixture over 2 min. After 10 min, the crude product was precipitated by adding CH_3OH (40 mL). The precipitate was separated and washed with H_2O (excess) and *n*-hexane (4×10 mL) to remove residual diamine. The crude was allowed to dry in the glass frit before being dissolved in a minimum volume of $CHCl_3$:acetone (8:2, *v/v*) with excess TBACl added as a solubilising agent and loaded onto a prep-TLC plate, which was run in an eluent system of $CHCl_3$:acetone (8:2, *v/v*). The silica containing the separated UV-active spot of the Cl$^-$ complex was collected and stirred in a system of CH_2Cl_2:acetone (7:3, *v/v*) for a minimum of 12 h before being filtered and evaporated under reduced pressure. The solid was collected, and anion exchange was then performed by suspending the solid in CH_3CN (150 mL), KPF_6 (10 equivs.) was added, and the mixture was stirred for 12 h. The bright white powdery solid was filtered and washed with H_2O (excess) before being dried *in vacuo*, with a final yield of 0.02826 g (4%).

^{1}H-NMR (600 MHz, DMSO-d_6): δ 10.34 (s, 4H), 8.58 (s, 2H), 8.00 (d, *J* = 8.9 Hz, 4H), 7.88 (dd, *J* = 6.0, 3.7 Hz, 4H), 7.36 (dd, *J* = 6.1, 3.5 Hz, 4H). **^{13}C{^{1}H}-NMR** (151 MHz, DMSO-d_6): δ 163.8, 162.0 (d, $^{1}J_{CF}$ = 245 Hz), 137.2, 137.1, 130.6, 126.0, 125.2, 122.8, 117.8, 117.7. **^{19}F-NMR** (471 MHz, DMSO-d_6): δ −112.7. **LR-MS** (ESI$^-$): [M+Cl]$^-$: 547.1 *m/z*. **HR-MS** (ESI$^+$) calculated for

$C_{28}H_{18}F_2N_4NaO_4$ $[M+Na]^+$: 535.11883 *m/z*, found: 535.11888 *m/z*. **M.P.**: >315 °C (decomp.). **R_f**: 0.42 in $CHCl_3$:acetone (8:2, *v/v*).

4^5,10^5-Difluoro-2,6,8,12-tetraaza-1,7(2,3)-dinaphthalena-4,10(1,3)-dibenzenacyclododecaphane-3,5,9,11-tetraone (Tetralactam 2b)

The reaction flask containing the 5-fluoroisophthaloyl dichloride (0.59968 g) was evacuated and charged with dry $N_{2(g)}$. The pre-dried TBACl (3.77046 g, 5 equivs.) was pre-dissolved in CH_2Cl_2 (20 mL). The CH_2Cl_2:TBACl solution (10 mL) was added directly to the reaction flask and allowed to stir for 10 min. The 2,3-diaminonapthalene (0.47181 g, 1.1 equivs.) was pre-dissolved in the CH_2Cl_2:TBACl solution (10 mL) and then added to the reaction mixture over 2 min. After 10 min, the crude product was precipitated by adding CH_3OH (40 mL). The precipitate was separated and washed with H_2O (excess) and *n*-hexane (4×10 mL) to remove residual diamine. The crude was allowed to dry in the glass frit before being dissolved in a minimum volume of $CHCl_3$:acetone (8:2, *v/v*) with excess TBACl added as a solubilising agent and loaded onto a prep-TLC plate, which was run in an eluent system of $CHCl_3$:acetone (8:2, *v/v*). The silica containing the separated UV-active spot of the Cl^- complex was collected and stirred in a system of CH_2Cl_2:acetone (7:3, *v/v*) for a minimum of 12 h before being filtered and evaporated under reduced pressure. The solid was collected, and anion exchange was then performed by suspending the solid in CH_3CN (150 mL), KPF_6 (10 equivs.) was added, and the mixture was stirred for 12 h. The light-tan solid was filtered and washed with H_2O (excess) before being dried *in vacuo*, with a final yield of 0.18616 g (11%).

^{1}H-NMR (600 MHz, DMSO-d_6): δ 10.43 (s, 4H), 8.68 (s, 2H), 8.47 (s, 4H), 8.03 (d, *J* = 8.9 Hz, 4H), 7.97 (d, *J* = 5.4 Hz, 4H), 7.26–7.67 (m, 4H). **^{13}C{^{1}H}-NMR** (201 MHz, DMSO-d_6): δ 163.8, 162.3 (d, $^1J_{CF}$ = 245 Hz), 136.8, 130.7, 129.3, 127.3, 126.1, 123.7, 122.8, 118.3 (d). **^{19}F-NMR** (471 MHz, DMSO-d_6): δ −112.7. **LR-MS** (ESI^-): $[M-H]^-$ and $[M+Cl]^-$: 611.3 and 647.3 *m/z*, respectively. **HR-MS** (ESI^-) calculated for $C_{36}H_{21}F_2N_4O_4$ $[M-H]^-$: 611.15364 *m/z*, found: 611.14369 *m/z*. **M.P.**: >338 °C (decomp.). **R_f**: 0.51 in $CHCl_3$:acetone (8:2, *v/v*).

1^4,1^5,4^5,7^4,7^5,10^5-Hexafluoro-2,6,8,12-tetraaza-1,7(1,2),4,10(1,3)-tetrabenzenacyclododecaphane-3,5,9,11-tetraone (Tetralactam 2c)

The reaction flask containing the 5-fluoroisophthaloyl dichloride (0.60008 g) was evacuated and charged with dry $N_{2(g)}$. The pre-dried TBACl (3.7730 g, 5 equivs.) was pre-dissolved in CH_2Cl_2 (20 mL). The CH_2Cl_2:TBACl solution (10 mL) was added directly to the reaction flask and allowed to stir for 10 min. The 1,2-diamino-4,5-difluorobenzene (0.43045 g, 1.1 equivs.) was also pre-dissolved in the CH_2Cl_2:TBACl solution (10 mL) and then added to the reaction mixture over 2 min. After 10 min, the crude product was precipitated by adding CH_3OH (40 mL). The precipitate was separated and washed with H_2O (excess) and *n*-hexane (4×10 mL) to remove residual diamine. The crude was allowed to dry in the glass frit before being dissolved in a mixture of $CHCl_3$:acetone (8:2, *v/v*) with excess TBACl added as a solubilising agent and loaded onto a prep-TLC plate, which was run in an eluent system of $CHCl_3$:acetone (8:2, *v/v*). The silica containing the separated UV-active spot of the Cl^- complex was collected and stirred in a system of CH_2Cl_2:acetone (7:3, *v/v*) for a minimum of 12 h before being filtered and evaporated under reduced pressure. The solid was collected, and anion exchange was then performed by suspending the solid in CH_3CN (150 mL), KPF_6 (10 equivs.) was added, and the mixture was stirred for 12 h. The off-white solid was filtered and washed with H_2O (excess) before being dried *in vacuo*, with a final yield of 0.01837 g (1%).

^{1}H-NMR (500 MHz, DMSO-d_6): δ 10.28 (s, 4H), 8.59 (s, 2H), 8.02 (t, *J* = 10.3 Hz, 4H), 7.97 (dd, *J* = 9.0, 1.4 Hz, 4H). **^{13}C{^{1}H}-NMR** (151 MHz, DMSO-d_6): δ 164.5, 161.9, 146.6 (d, $^1J_{CF}$ = 245 Hz), 137.3, 127.8, 123.4, 118.5 (d), 114.1. **^{19}F-NMR** (471 MHz, DMSO-d_6): δ −112.6, −141.2. **LR-MS** (ESI^-): $[M-H]^-$: 583.2 *m/z*. **HR-MS** (ESI^-) calculated for $C_{28}H_{13}F_6N_4O_4$ $[M-H]^-$: 583.08465 *m/z*, found: 583.08447 *m/z*. **M.P.**: >294 °C (decomp.). **R_f**: 0.37 in $CHCl_3$:acetone (8:2, *v/v*).

4^5,10^5-Bis(trifluoromethyl)-2,6,8,12-tetraaza-1,7(1,2),4,10(1,3)-tetrabenzenacyclododecaphane-3,5,9,11-tetraone (Tetralactam 3a)

The reaction flask containing the 5-(trifluoromethyl)isophthaloyl dichloride (0.60565 g) was evacuated and charged with dry $N_{2(g)}$. The pre-dried TBACl (3.10534 g, 5 equivs.) was pre-dissolved in CH_2Cl_2 (20 mL). The CH_2Cl_2:TBACl solution (10 mL) was added directly to the reaction flask and allowed to stir for 10 min. The *ortho*-phenylenediamine (0.26567 g, 1.1 equivs.) was pre-dissolved in the CH_2Cl_2:TBACl solution (10 mL) and then added to the reaction mixture over 2 min. After 10 min, the crude product was precipitated by adding CH_3OH (40 mL). The precipitate was separated and washed with H_2O (excess) and *n*-hexane (4×10 mL) to remove residual diamine. The crude was then triturated in $CHCl_3$:acetone (8:2, *v/v*, 10 mL), after which the solution was allowed to stand at r.t. while the Cl^- complex slowly precipitated. Once at r.t., the solid was separated from the trituration mixture and washed again with water (excess) and *n*-hexane (4×10 mL). The filtrate was also collected, and the trituration process was repeated until no more solid precipitated from the solution. The collected solids were consolidated, and anion exchange was then performed by suspending the solid in CH_3CN (150 mL), KPF_6 (10 equivs.) was added, and the mixture was stirred for 12 h. The white solid was filtered and washed with H_2O (excess) before being dried *in vacuo*, with a final yield of 0.53959 g (39%).

^{1}H-NMR (500 MHz, DMSO-d_6): δ 10.47 (s, 4H), 9.04 (s, 2H), 8.48 (s, 4H), 7.92 (dd, J = 6.1, 3.6 Hz, 4H), 7.37 (dd, J = 6.2, 3.6 Hz, 4H). **^{13}C{^{1}H}-NMR** (201 MHz, DMSO-d_6): δ 163.6, 135.6, 130.5, 129.9 (q, $^{2}J_{CF}$ = 33 Hz), 127.7, 125.8, 125.6, 123.6 (q, $^{1}J_{CF}$ = 272 Hz). **^{19}F-NMR** (471 MHz, DMSO-d_6): δ −62.60. **LR-MS** (ESI$^+$): [M+Na]$^+$: 635.1 *m/z*, (ESI$^-$): [M−H]$^-$ and [M+Cl]$^-$: 611.2 and 647.2 *m/z*, respectively. **HR-MS** (ESI$^+$) calculated for $C_{30}H_{18}F_6N_4NaO_4$ [M+Na]$^+$: 635.11244 *m/z*, found: 635.11286 *m/z*. **M.P.**: >305 °C (decomp.).

4^5,10^5-Bis(trifluoromethyl)-2,6,8,12-tetraaza-1,7(2,3)-dinaphthalena-4,10(1,3)-dibenzenacyclododecaphane-3,5,9,11-tetraone (Tetralactam 3b)

The reaction flask containing the 5-(trifluoromethyl)isophthaloyl dichloride (0.55408 g) was evacuated and charged with dry $N_{2(g)}$. The pre-dried TBACl (2.97126 g, 5 equivs.) was pre-dissolved in CH_2Cl_2 (20 mL). The CH_2Cl_2:TBACl solution (10 mL) was added directly to the reaction flask and allowed to stir for 10 min. The 2,3-diaminonapthalene (0.37181 g, 1.1 equivs.) was pre-dissolved in the CH_2Cl_2:TBACl solution (10 mL) and then added to the reaction mixture over 2 min. After 10 min, the crude product was precipitated by adding CH_3OH (40 mL). The precipitate was separated and washed with H_2O (excess) and *n*-hexane (4×10 mL) to remove residual diamine. The crude was then triturated in CH_2Cl_2 (8:2, *v/v*, 10 mL), after which the solution was allowed to stand at r.t. while the Cl^- complex slowly precipitated. Once at r.t., the solid was separated from the trituration mixture and washed again with water (excess) and *n*-hexane (4×10 mL). The filtrate was also collected, and the trituration process was repeated until no more solid precipitated from the solution. The collected solids were consolidated, and anion exchange was then performed by suspending the solid in CH_3CN (150 mL), KPF_6 (10 equivs.) was added, and the mixture was stirred for 12 h. The off-white solid was filtered and washed with H_2O (excess) before being dried *in vacuo*, with a final yield of 0.02040 g (1%).

^{1}H-NMR (500 MHz, DMSO-d_6): δ 10.55 (s, 4H), 9.04 (s, 2H), 8.49 (s, 4H), 8.54 (s, 4H), 7.99 (dd, J = 6.2, 3.3 Hz, 4H), 7.57 (dd, J = 6.2, 3.2 Hz, 4H). **^{13}C{^{1}H}-NMR** (201 MHz, DMSO-d_6): δ 163.9, 135.6, 130.8, 130.6, 130.0, 129.9 (q, $^{2}J_{CF}$ = 33 Hz), 129.3, 127.8, 127.4, 126.2, 123.7, 123.6 (q, $^{1}J_{CF}$ = 272 Hz). **^{19}F-NMR** (471 MHz, DMSO-d_6): δ −62.6. **LR-MS** (ESI$^+$): [M+Na]$^+$: 735.1 *m/z*, (ESI$^-$): [M−H]$^-$: 711.2 *m/z*. **HR-MS** (ESI$^+$) calculated for $C_{38}H_{22}F_6N_4NaO_4$ [M+Na]$^+$: 735.14374 *m/z*, found: 735.14379 *m/z*. **M.P.**: >250 °C (decomp.).

1^4,1^5,7^4,7^5-Tetrafluoro-4^5,10^5-bis(trifluoromethyl)-2,6,8,12-tetraaza-1,7(1,2),4,10(1,3)-tetrabenzenacyclododecaphane-3,5,9,11-tetraone (Tetralactam 3c)

The reaction flask containing the 5-(trifluoromethyl)isophthaloyl dichloride (0.20250 g) was evacuated and charged with dry $N_{2(g)}$. The pre-dried TBACl (1.08590 g, 5 equivs.) was pre-dissolved in CH_2Cl_2 (20 mL). The CH_2Cl_2:TBACl solution (10 mL) was added directly to the reaction flask and allowed to stir for 10 min. The 1,2-diamino-4,5-difluorobenzene (0.12388 g, 1.1 equivs.) was also pre-dissolved in the CH_2Cl_2:TBACl solution (10 mL) and then added to the reaction mixture over 2 min. After a total of 10 min, the reaction was stopped, and the volatiles evaporated under reduced pressure. The crude material was then triturated in hot acetone (55 °C, 328.15 K). The mixture was allowed to cool to r.t. before being placed in the freezer at −20 °C (253.15 K), where a white precipitate of the Cl^- complex formed over 48 h. The precipitate was separated and washed with H_2O (excess) and *n*-hexane (4×10 mL) to remove residual diamine and excess TBACl. The filtrate was also collected, and the trituration process was repeated until no more solid precipitated from the solution. The collected solids were consolidated, and anion exchange was then performed by suspending the solid in CH_3CN (25 mL), KPF_6 (10 equivs.) was added, and the mixture was stirred for 12 h. The fine purple solid was filtered and washed with H_2O (excess) before being dried *in vacuo*, with a final yield of 0.04066 g (8%).

^{1}H-NMR (800 MHz, DMSO-d_6): δ 10.77 (s, 4H), 10.03 (s, 2H), 8.39 (s, 4H), 8.08 (t, J = 10.4 Hz, 4H). **^{13}C{^{1}H}-NMR** (201 MHz, DMSO-d_6): δ 163.7, 146.0 (dd, $^{1}J_{CF}$ = 245 Hz, $^{2}J_{CF}$ = 17 Hz), 134.9, 130.7, 129.9 (q, $^{2}J_{CF}$ = 32 Hz), 128.1, 127.0, 123.5 (q, $^{1}J_{CF}$ = 272 Hz), 114.4 (d, $^{2}J_{CF}$ = 15 Hz). **^{19}F-NMR** (471 MHz, DMSO-d_6): δ −62.69, −141.16. **LR-MS** (ESI$^+$): [M+Na]$^+$: 707.0 *m/z*, (ESI$^-$): [M−H]$^-$: 683.1 *m/z*. **HR-MS** (ESI$^+$) calculated for $C_{30}H_{14}F_{10}N_4NaO_4$ [M+Na]$^+$: 707.07476 *m/z*, found: 707.07458 *m/z*. **M.P.**: 383–397 °C.

4^5,10^5-Di-*tert*-butyl-2,6,8,12-tetraaza-1,7(1,2),4,10(1,3)-tetrabenzenacyclododecaphane-3,5,9,11-tetraone (Tetralactam 4a)

Tetralactam **4a** was synthesised according to an adapted previously reported method.[22] The TBACl (1.8890 g, 5 equivs.) was dried in vacuo for 1 h and dissolved in CH_2Cl_2 (30 mL, dry, degassed). First, the *ortho*-phenylenediamine (92.5 mg, 1.1 equivs.) was dissolved in CH_2Cl_2 (15 mL). The CH_2Cl_2:TBACl solution was added dropwise to the 5-*tert*-butylisophthaloyl dichloride (0.2017 g) under $N_{2(g)}$, and more CH_2Cl_2 (30 mL, dry, degassed) was added and allowed to stir for 0.5 h to ensure homogeneity. The reaction flask was re-evacuated with $N_{2(g)}$ before the diamine solution was added via syringe over 2 min. The reaction was allowed to stir for an extra 8 min before the reaction stopped, and the volatiles were removed under reduced pressure. The solid was then suspended in H_2O (50 mL) and sonicated before a system of CH_3CN:H_2O (3:7, *v/v*) was added to the agitated mixture and cooled to 4 °C (277.15 K), produced to precipitate the crude product. The precipitate was then triturated in $CHCl_3$ (100 mL, 60 °C), and the mixture was cooled to produce the chloride complex. The floating solid was collected, and anion

exchange was then performed by resuspending the solid in H_2O (150 mL) with KPF_6 (10 equivs.) and stirred for 12 h. The solid was then filtered and washed with H_2O (excess). The solid was dried *in vacuo*, resulting in a final yield of the white solid was 0.08155 g (18%).

^{1}H-NMR (500 MHz, DMSO-d_6): δ 10.25 (s, 4H), 8.56 (t, J = 1.6 Hz, 2H), 8.22 (d, J = 1.6 Hz, 4H), 7.90 (dd, J = 6.0, 3.6 Hz, 4H), 7.36 (dd, J = 6.1, 3.5 Hz, 4H), 1.40 (s, 18H). **^{13}C{^{1}H}-NMR** (126 MHz, DMSO-d_6): δ 165.1, 152.0, 134.5, 130.8, 127.7, 125.8, 125.1, 123.6, 34.9, 30.9. **LR-MS** (ESI$^-$): $[M-H]^-$ and $[M+Cl]^-$: 587.4 and 623.3 *m/z*, respectively. **HR-MS** (ESI$^+$) calculated for $C_{36}H_{36}N_4NaO_4$ $[M+Na]^+$: 611.26288 *m/z*, found: 611.26292 *m/z*. **M.P.**: 362–378 °C.

4^5,10^5-Di-*tert*-butyl-2,6,8,12-tetraaza-1,7(2,3)-dinaphthalena-4,10(1,3)-dibenzenacyclododecaphane-3,5,9,11-tetraone (Tetralactam 4b)
The reaction flask containing the 5-*tert*-butylisophthaloyl dichloride (0.06949 g) was evacuated and charged with dry $N_{2(g)}$. The pre-dried TBACl (0.35635 g, 5 equivs.) was pre-dissolved in CH_2Cl_2 (20 mL). The CH_2Cl_2:TBACl solution (10 mL) was added directly to the reaction flask and allowed to stir for 10 min. The 2,3-diaminonapthalene (0.04459 g, 1.1 equivs.) was pre-dissolved in the CH_2Cl_2:TBACl solution (10 mL) and then added to the reaction mixture over 2 min. After a total of 10 min, the reaction was stopped, and the volatiles evaporated under reduced pressure. A system of *n*-hexane:CH_3OH (8:2, *v/v*) was added to the crude solid, producing a brown precipitate formed at the interface between the solvents. This process was repeated until precipitation stopped. The collected solids were then dissolved in a mixture of CH_2Cl_2:CH_3OH (2:1, *v/v*, 20 mL) and cooled to –20 °C for 24 h. The Cl^- complex of the desired product was separated and resuspended in CH_3OH (−20 °C, 10 mL) for 12 h before the solid was collected and dried. Anion exchange was then performed by suspending the solid in CH_3CN (25 mL), KPF_6 (10 equivs.) was added, and the mixture was stirred for 12 h. The fine purple solid was filtered and washed with H_2O (excess) before being dried *in vacuo*, with a final yield of 0.02633 g (15%).

^{1}H-NMR (600 MHz, DMSO-d_6): δ 10.40 (s, 4H), 8.69 (s, 2H), 8.50 (s, 4H), 8.27 (s, 4H), 8.04–7.91 (app. s, 4H), 7.58–7.51 (app. s, 4H), 1.43 (s, 18H). **^{13}C{^{1}H}-NMR** (151 MHz, DMSO-d_6): δ 165.8, 152.1, 134.7, 130.8, 130.0, 127.9, 127.3, 126.2, 123.8, 122.7, 35.0, 31.0. **LR-MS** (ESI$^-$): $[M-H]^-$ and $[M+Cl]^-$: 687.4 and 723.3 *m/z*, respectively. **HR-MS** (ESI$^+$) calculated for $C_{44}H_{40}N_4NaO_4$ $[M+Na]^+$: 711.29418 *m/z*, found: 711.29445 *m/z*. **M.P.**: >388 °C (decomp.).

4^5,10^5-Di-*tert*-butyl-1^4,1^5,7^4,7^5-tetrafluoro-2,6,8,12-tetraaza-1,7(1,2),4,10(1,3)-tetrabenzenacyclododecaphane-3,5,9,11-tetraone (Tetralactam 4c)
The reaction flask containing the 5-*tert*-butylisophthaloyl dichloride (0.62662 g) was evacuated and charged with dry $N_{2(g)}$. The pre-dried TBACl (3.21289 g, 5 equivs.) was pre-dissolved in CH_2Cl_2 (20 mL). The CH_2Cl_2:TBACl solution (10 mL) was added directly to the reaction flask and allowed to stir for 10 min. The 1,2-diamino-4,5-difluorobenzene (0.36654 g, 1.1 equivs.) was also pre-dissolved in the CH_2Cl_2:TBACl solution (10 mL) and then added to the reaction mixture over 2 min. After a total of 10 min, the reaction was stopped, and the volatiles evaporated under reduced pressure H_2O (15 mL) was added to the viscous oil-like crude material, and then a mixture of CH_3CN:H_2O (3:7, *v/v*, 35 mL) was added to the aqueous mixture causing a brown solid to precipitate. The solid was separated, and the H_2O content of the filtrate increased by 10 mL until no more precipitate was observed. The collected solids were then triturated in CH_3OH (25 mL) and cooled to –20 °C for two weeks. The Cl^- complex of the desired product was separated and dried. Anion exchange was then performed by suspending the solid in CH_3CN (25 mL), KPF_6 (10 equivs.) was added, and the mixture was stirred for 12 h. The fine mauve solid was then filtered and washed with H_2O (excess) before being dried *in vacuo*, with a final yield of 0.00552 g (<1%).

^{1}H-NMR (600 MHz, DMSO-d_6): δ 10.20 (s, 4H), 8.61 (s, 2H), 8.18 (d, J = 1.5 Hz, 4H), 8.07 (t, J = 10.4 Hz, 4H), 1.38 (s, 18H). **^{13}C{^{1}H}-NMR** (151 MHz, DMSO-d_6): δ 165.5, 152.1, 146.0 (dd, $^1J_{CF}$ = 245 Hz, $^2J_{CF}$ = 15 Hz), 134.3, 128.1, 127.4, 123.7, 113.6, 34.9, 30.9. **^{19}F-NMR** (471 MHz, DMSO-d_6): δ −141.7. **LR-MS** (ESI$^-$): $[M-H]^-$: 659.3 *m/z*. **HR-MS** (ESI$^+$) calculated for $C_{36}H_{32}F_4N_4NaO_4$ $[M+Na]^+$: 683.22519 *m/z*, found: 683.22527 *m/z*. **M.P.**: 368–381 °C.

5-Fluoro-*N*^{1},*N*^{3}-diphenylisophthalamide (Isophthalamide 5)
5-Fluoroisophthaloyl dichloride (0.60192 g) was prepared using a previously reported method,[27] which was then dissolved in CH_2Cl_2 and stirred while the system was purged with $N_{2(g)}$ for 10 min. Aniline (0.5703 mL, 0.55801 g, 2.2 equivs.) was added in slight excess dropwise over 30 s, where the solution turned translucent yellow to deep California brick red as a precipitate began to form. The reaction was allowed to stir for 2.5 h at r.t. after which the precipitate was filtered, and the light-cream-coloured solid was washed with CH_2Cl_2 (3×10 mL) and *n*-hexane (excess). The solid was then resuspended in $CHCl_3$ (60 mL) and washed with H_2O (3×60 mL) before HCl (1 M, 1 mL) was added to the aqueous phase of the third wash. The organic phase was collected and dried over $MgSO_4$ (Anhyd.) before filtration and evaporation under reduced pressure. The white solid was dried for 12 h *in vacuo*, resulting in the isolation of **5** with a final yield of 0.46285 g (51%).

^{1}H-NMR (500 MHz, DMSO-d_6): δ 10.47 (s, 2H), 8.41 (t, J = 1.5 Hz, 1H), 7.99 (dd, J = 9.2, 1.5 Hz, 2H), 7.71–7.86 (m, 4H), 7.35–7.43 (m, 4H), 7.14 (tt, J = 7.3, 1.2 Hz, 2H). **^{13}C{^{1}H}-NMR** (126 MHz, DMSO-d_6): δ 163.6, 161.6 (d, $^{1}J_{CF}$ = 245 Hz), 138.8, 137.4 (d, $^{3}J_{CF}$ = 6.7 Hz), 128.7, 124.1, 123.2, 120.4, 117.5 (d, $^{2}J_{CF}$ = 23 Hz). **^{19}F-NMR** (471 MHz, DMSO-d_6): δ −113.5. **LR-MS** (ESI$^-$): [M−H]$^-$ and [M+Cl]$^-$: 333.1 and 369.1 *m/z*, respectively. **HR-MS** (ESI$^+$) calculated for $C_{20}H_{15}FN_2NaO_2$ [M+Na]$^+$: 357.10098 *m/z*, found: 357.10105 *m/z*. **M.P.**: 286–290 °C.

3-Fluoro-*N*-[2-[(3-fluorobenzoyl)amino]phenyl]benzamide (Benzamide 6)

Benzamide **6** was synthesised according to previously reported methods. First dissolving *ortho*-phenylenediamine (1.0039 g) in CH_2Cl_2 (50 mL).[28] The reaction mixture was cooled to 0 °C over an ice bath. Dropwise addition of 3-fluorobenzoyl chloride (2.26 mL, ~2 equivs.) to the reaction mixture over 5 min resulted in an immediate bubbling exothermic reaction as $HCl_{(g)}$ was generated while the desired product began to precipitate as a light pink solid (which was quite aromatic and smelt like bananas when filtered later in the reaction). As the reaction progressed, it was especially important to ensure that outgassing could easily occur to reduce any built-up system pressure. After 2.5 h, the precipitate was separated, washed with CH_2Cl_2 (0 °C, 2×10 mL) and H_2O (2×10 mL), and dried *in vacuo* for 12 h. The desired product was isolated as a white solid with a final yield of 1.0894 g (33%).

^{1}H-NMR (500 MHz, DMSO-d_6): δ 10.07 (s, 2H), 7.79 (dt, J = 7.7, 1.2 Hz, 2H), 7.74 (ddd, J = 9.9, 2.7, 1.6 Hz, 2H), 7.65 (dt, J = 7.4, 3.7 Hz, 2H), 7.57 (td, J = 8.0, 5.8 Hz, 2H), 7.44 (tdd, J = 8.5, 2.7, 1.0 Hz, 2H), 7.30 (dd, J = 6.1, 3.5 Hz, 2H). **^{13}C{^{1}H}-NMR** (126 MHz, DMSO-d_6): δ 164.2, 161.9 (d, $^{1}J_{CF}$ = 245 Hz), 136.7 ($^{3}J_{CF}$ = 6.9 Hz), 131.3, 130.7 (d, $^{3}J_{CF}$ = 8.1 Hz), 126.1, 125.7, 123.7 (d, $^{4}J_{CF}$ = 2.4 Hz), 118.6 (d, $^{2}J_{CF}$ = 21 Hz), 114.5 (d, $^{2}J_{CF}$ = 21 Hz). **^{19}F-NMR** (471 MHz, DMSO-d_6): δ −114.0. **LR-MS** (ESI$^-$): [M−H]$^-$ and [M+Cl]$^-$: 351.1 and 387.0 *m/z*, respectively. **HR-MS** (ESI$^+$) calculated for $C_{20}H_{14}F_2N_2NaO_2$ [M+Na]$^+$: 375.09155 *m/z*, found: 375.09156 *m/z*. **M.P.**: 229–233 °C.

^{1}H-NMR Binding Studies and Covariance of Fit Calculations

Host solutions of tetralactams **1a**–**4c** and acyclic compounds **5** and **6** (1 mM) were made up in DMSO-d_6/H_2O (0.5%). The same host solutions were then used to make the concentrated guest solution (1 M) containing the titrant guest anion (either Cl^- or F^-) as the TBA^+ salt. The host solution and the concentrated guest solution were then used to make a dilute guest solution (0.1 M). The titration experiments were initiated by first acquiring a ^{1}H-NMR spectrum of the host solution (0.5 mL) without any of the guest solutions added. Subsequent spectrums were acquired after each addition of the guest solutions. Initially, the dilute guest solution was added slowly until 10 equivs. of the guest anion was achieved. Further guest anion additions were done using the concentrated guest solution and only stopped after the interacting ^{1}H-NMR peaks of the host stopped shifting at ~400–600 Equivs. of the guest. The changing chemical shifts (ppm) of the resonances attributed to the protons of the host were first referenced to the DMSO-d_6 proton peak at 2.50 ppm used as the internal standard and then tracked and inputted into the BindFit web applet from www.supramolecular.org to produce host:guest binding constants (K_a).[29,30]

The Cl^-/NO_3^- Exchange Assay and Hill Analysis

The assay was performed using synthetic large unilamellar vesicles (200 nm) formed from POPC, which were rehydrated with an internal solution of NaCl (489 mM), and a phosphate buffer formed by Na_2HPO_4 (5 mM) and $NaH_2PO_4{\cdot}2H_2O$ (5 mM).[32,46] The vesicles then underwent nine freeze-thaw cycles. Once the vesicles had thawed to r.t., they were extruded through a 200 nm polycarbonate membrane twenty-five times and then dialysed in a phosphate buffer solution for 12 h to remove any residual unencapsulated Cl^-. An external solution of $NaNO_3$ (489 mM) was then made using the same phosphate buffer solution (5 mM), and both the internal and external solutions were adjusted to pH 7.2. The assay was prepared by first adding the vesicles (1 mM) into 5 mL of the external solution. Anion transport was initiated at t = 0 s by adding each tetralactam as a DMSO solution (10 μL), and the subsequent Cl^- efflux was recorded using the ISE. The 100% Cl^- efflux value required for data calibration was obtained by lysing the vesicles with Triton X−100 (50 μL, 10%, *v/v*) detergent at t = 300 s after which a further 120 s of data was collected before the transport experiment was stopped at t = 420 s. The recorded data was then calibrated to the obtained 100% Cl^- efflux value recorded after t = 300 s. Each transport experiment at each receptor concentration was performed at least twice. If the transporters were soluble enough to be tested at a range of different concentrations, the collected datasets underwent Hill analysis to obtain the EC_{50} values and the Hill coefficients (n).

First, the calibrated transport data at t = 270 s of each tested transporter concentration (mol%) was plotted against the normalised percentage Cl^- efflux (%) for ISE-based transport studies. For spectrophotometer fluorescence- or luminescence-based transport studies, the normalised fractional fluorescence or luminescence intensity (I_f) data at either t = 200 s or t = 600 s, respectively, was graphed against the tested transporter concentration (mol%). The graphed data was then fitted using the Hill equation (Equation 1):

$$y = y_0 + (y_1 - y_0) \times \frac{x^n}{(k^n + x^n)}$$

Equation 1: The Hill equation which was used to derive EC_{50} values and Hill coefficients (*n*).
Where *x* is the concentration of the transporter (mol%), *y* is the Cl^- efflux (%) at *t* = 270 s, the I_f value at *t* = 200 s for fluorescence-based studies, and *t* = 600 s for luminescence-based studies, y_0 is the minimum Cl^- efflux (%) or I_f value, y_1 is the Cl^- efflux (%) or I_f value at time *t*, *k* is the EC_{50} value in mol%, and *n* is the Hill coefficient.

The Cationophore Coupled Transport Assay and Initial Rate Constant Calculations
Synthetic vesicles (200 nm) were made using the same initial process as described for the Cl^-/NO_3^- exchange assay, except the vesicles were made to contain an internal solution of KCl (300 mM) or KF (300 mM) and were suspended in an external solution of K-Gluc (300 mM).[32,33] Both the internal and external solutions were buffered to pH 7.2 using HEPES (10 mM). Depending on which transport method was being assessed, either the ionophore Vln, to study electrogenic transport, or the ionophore Mon, to study electroneutral transport (0.1 mol%, 10 µL, as DMSO solutions) were added to the system of vesicles (1 mM, with a final assay volume of 5 mL) at *t* = −30 s. Fresh DMSO solutions of each tetralactam (0.05 mol% or 0.0005 mol% for **3c**) were made, and 10 µL was added to the assay system at *t* = 0 s to initiate anion transport. Each transport experiment continued until *t* = 300 s, where Triton X-100 (50 µL, 10% *v/v*) was added to lyse the vesicles. Each experiment continued until *t* = 420 s to record the value 100% Cl^- efflux, using a Cl^- ISE, or 100% F^- efflux, using a F^- ISE, which was necessary to calibrate the recorded data. Each transport experiment was performed at least twice to obtain standard errors. A control experiment was also performed using pure DMSO to ensure no transport was being observed without transporters. Note that if F^- transport is being tested, Vln is the only ionophore that can be added to assess electrogenic F^- uniport; if Mon is added to try and analyse H^+/F^- co-transport, uncontrolled HF transport will occur. The calibrated anion efflux (%) data recorded for each transporter was then graphed as a function of time before being fitted to a two-phase exponential decay function (Equation 2) to derive initial rate constants (k_{ini}, s^{-1}).

$$y = y_0 + A_1 e^{\left(\frac{-x}{t_1}\right)} + A_2 e^{\left(\frac{-x}{t_2}\right)}$$

Equation 2: The two-phase exponential decay function used to derive the amplitude and time constants required to calculate initial rates.
Where *y* is the Cl^- or F^- efflux (%) normalised against the 100% anion efflux value, y_0 is the offset of the fitted non-linear curve to the experimental data, A_1 and A_2 are the first and second amplitude constants, respectively, *x* is time *t*, and t_1 and t_2 are the first and second time constants, respectively, which are derived during the data fitting process. The generated amplitude (A_1 and A_2) and time (t_1 and t_2) constants are then used to find the k_{ini} rate constant using Equation 3:

$$k_{ini} = \left(\frac{dy}{dx}\right) x = 0 = -\frac{A_1}{t_1} - \frac{A_2}{t_2}$$

Equation 3: The initial rate constant equation used to derive k_{ini} (s^{-1}) values from the amplitude and time constants.
However, in the case of very low transport rates preventing the data from being accurately fitted to a non-linear curve, the data can be fitted using linear regression with Equation 4:

$$y = a + bx$$

Equation 4: The linear equation used during linear regression fitting.
Where *y* is the normalised Cl^- or F^- efflux (%) value, *a* is the intercept of the x-axis intercept (the value of *y* when *x* (time *t*, in s) equals 0, and *b* is the slope of the fitted line which is equal to the k_{ini} rate constant (s^{-1}).

The HPTS Transport Selectivity Assay
Synthetic POPC vesicles (200 nm) containing NaCl (100 mM), HEPES (10 mM), and HPTS (1 mM) were made using a similar initial method as described for the ISE-based assays.[34] However, after the freeze-thaw cycles and twenty-five extrusions, the unencapsulated internal solution was removed via size-exclusion chromatography using G-25 Sephadex® beads, which had first been cleaned by eluting the external solution through the column. The external solution also consisted of NaCl (100 mM) and HEPES (10 mM), and both the internal and external solutions were adjusted to pH 7. The vesicles were collected after size separation and diluted to a known concentration. During the transport experiments, the spectrophotometer excited the HPTS probe at λ_{ex} = 403 nm (to excite the protonated form) and λ_{ex} = 460 nm (to excite the deprotonated form), with the fluorescence emission of both being monitored at an emission wavelength of λ_{em} = 510 nm. Transport studies were first set up by adding the vesicles (0.1 mM) to a cuvette containing the external solution (2.5 mL). A base pulse of NaOH (0.5 M, 25 µL) was then added at *t* = −30 s to raise the pH of the external solution by ~1 unit. After confirming no vesicle leakage was occurring, the transporters were added as DMSO solutions (5 µL) at *t* = 0 s to initiate transport. Transport was allowed to continue until *t* = 230 s, where Triton X-100 (50 µL, 10%, *v/v*) was added to lyse the vesicles and obtain the 100% fractional fluorescence intensity (I_f) reading. The experiments were stopped at *t* = 280 s, and each experiment for each transporter concentration was repeated twice to obtain standard errors. The vesicles could also be treated with CCCP (1 mol%) before the addition of the base pulse to study transporter-mediated Cl^- uniport. Vesicles could also be pretreated using BSA (1 mol%) to remove all membrane-bound fatty acids and determine the possibility of transporter-mediated H^+/Cl^- co-transport unaided by the fatty acid flip-flop mechanism.

The data obtained from these experiments was first calibrated to the 100% fractional fluorescence intensity (I_f) reading, and then the data at t = 200 s was graphed as a function of transporter concentration and fitted to the Hill equation (Equation 1) to derive Hill coefficients and EC_{50} values.

The Adjusted HPTS Transport Assay

The adjusted HPTS assay uses synthetic EYPC vesicles that are made in the same way as those used for the HPTS transport selectivity assay, apart from being made from EYPC rather than POPC, 100 nm in size instead of 200 nm, and the intra- and extra-vesicular solutions were buffered to pH 7.2 instead of pH 7.0.[21] The modified assay also used a single excitation wavelength at 450 nm to excite the pH-sensitive fluorescent HPTS probe and recorded fluorescence emission data at a wavelength of 510 nm, instead of a dual excitation wavelength. Also, compared to the 30 s leakage check performed for the HPTS transport selectivity assay, the modified assay performs a 100 s leakage check after the NaOH base pulse was added. At t = 100 s, the transporters were then added as DMSO solutions, with each transport experiment continuing for a further 200 s, after which vesicle lysis occurred to record the 100% Cl^- efflux value for data normalisation. The data collection of each transport experiment was stopped at t = 270 s, and the fluorescence data was normalised to the 100% fluorescence emission value before being fitted to the Hill equation (Equation 1) to derive Hill coefficients and EC_{50} values.

The HPTS Anion Gradient Assay

Synthetic POPC vesicles (200 nm) containing NaCl (100 mM), HEPES (10 mM), and HPTS (1 mM) were made using the same method described in the HPTS transport selectivity assay.[39] However, the vesicles were suspended in different external solutions containing the anion of interest as NaX salts (X = Cl^-, Br^-, NO_3^-, I^-, and ClO_4^-). No base pulse was added before transport was initiated by adding the transporters as DMSO solutions (5 μL) at t = 30 s. The transport experiments continued until the rate of transport plateaued or the fluorescence intensity reached an inflexion point. Before pH data could be obtained from the recorded fluorescence data, a calibration curve was constructed by using the same vesicles and conditions as the HPTS assay and monitoring the fluorescence intensity of the HPTS probe as the pH of the system was adjusted incrementally using a NaOH solution. The collected I_f data was then normalised and graphed as a function of the overall assay pH before the data was fitted with a modified Henderson-Hasselbach equation (Equation 5).

$$y = log\frac{ax - b}{c - x}$$

Equation 5: The Henderson-Hasselbach equation, which has been modified to determine pH.

Where y is the system pH, x is the I_f value, and a, b, and c are all constants which are derived during the data fitting process. These three constants are then used to calibrate the remaining fluorescence data obtained through the transport experiments. The experimental I_f values were substituted for term x in Equation 5 to derive the equivalent pH value, which was then used to calculate the change in the system pH using Equation 6.

$$\Delta pH = pH - pH_{INI}$$

Equation 6: The equation used to derive the change in system pH (ΔpH).

Where the ΔpH is the system, pH is derived pH at time t, and pH_{INI} is the pH value at the beginning of the experiment when t = 0 s.

The Eu(III) F^- Transport Assay

Vesicles were prepared using the same methods as those used during the HPTS assay; however, the concentrations of both NaCl (225 mM) and HEPES (0.5 mM) were changed.[42,43] Also, the internal solution contained probe the previously reported Eu(III) probe (50 μM). Both the internal and external solutions were buffered to pH 7.0. The spectrophotometer was set up such that the luminescence intensity at λ_{em} = 615 nm was recorded when the Eu(III) probe was excited at an excitation wavelength of λ_{ex} = 332 nm. Also, a 0.1 ms time-gate was added, producing a total acquisition time of 2 ms. The assay system was prepared by adding vesicles (0.4 mM) to quartz cuvettes containing the external solution (2.5 mL). An aqueous solution containing NaF (0.18 M), NaCl (225 mM), and HEPES (0.5 mM) was then added at t = 0 s as an ion pulse, resulting in a final NaF concentration of 3 mM. Like the HPTS assay, the vesicles were checked for leakage for 30 s before transport was initiated. At t = 30 s, the DMSO solutions of transporters at varied concentrations (5 μL) were added to the assay system to elicit transport, which was monitored over 600 s. At t = 630 s, the vesicles were lysed using Triton X-100 detergent to obtain the 100% efflux calibration value. Each transport experiment was stopped at t = 750 s, and each transport experiment performed for each tested transporter concentration was repeated twice to obtain standard errors. The data was then normalised and graphed as a function of time. The data at t = 600 s was graphed as a function of transporter concentration and then fitted to the Hill equation (Equation 1) to derive Hill coefficients and EC_{50} values.

Resource Availability

Lead Contact

Requests for any of the listed chemical reagents and resources should be addressed to the lead contact, Philip A. Gale (philip.gale@uts.edu.au).

Materials Availability

The syntheses of all reported compounds are described in the synthesis and characterization of compounds. Further information on synthesis and characterization is available in the electronic supplementary information document. If available, compounds **1a**–**4c** can be requested from the lead contact. All other chemical reagents used during synthesis, binding, or transport studies were bought from commercial suppliers or available from the School of Chemistry or the School of Pharmacy at The University of Sydney.

Data and Code Availability

- Data which has been reported in this work is available from the lead contact upon request.
- Crystallographic data have been deposited in the Cambridge Crystallographic Data Centre (CCDC) under accession numbers CCDC: 2358365 (**1b**·2Cl$^-$), CCDC: 2355823 (**2a**·Cl$^-$), CCDC: 2358370 (**2a**·F$^-$), CCDC: 2358369 (**2c**·Cl$^-$), CCDC: 2358367 (**3a**·Cl$^-$), CCDC: 2358860 (**3a**·F$^-$), CCDC: 2358372 (**3c**), CCDC: 2271744 (**4b**·Cl$^-$). The data can be obtained free of charge at https://www.ccdc.cam.ac.uk/structures/.
- No original code was used or reported in this work.
- Further information needed to reanalyze the data reported in this work is available from the lead contact upon request.

SUPPLEMENTAL INFORMATION

Document S1 is the main supplemental PDF:

Document S1. Supplemental experimental procedures and data, Figure S1–S177, and Table S1–S75.

ACKNOWLEDGMENTS

The authors acknowledge and pay respect to the Gadigal people of the Eora Nation, the traditional owners of the land on which we research, teach, and collaborate at The University of Technology Sydney and the University of Sydney. P.A.G. thanks the Australian Research Council (DP210100039) and the University of Technology Sydney for funding. A.M.G. would like to thank The University of Sydney and the Australian Government for the Research Training Program scholarship (RTP).

AUTHOR CONTRIBUTIONS

A.M.G. prepared the original manuscript and electronic supplementary information draft, synthesised and characterised the compounds, grew the single crystals, and performed the NMR binding and vesicle transport studies. D.A.M., X.W., D.E.H., and P.A.G. supervised the project. M.M., D.E.H., and B.A.H. performed the X-ray crystallographic analysis. S.J.B. assisted with the initial setup of the Eu(III) F$^-$ transport assay. X.W. assisted with the analysis of the vesicle studies data. P.A.G. conceptualised the project. All contributed to the editing of the final manuscript.

DECLARATION OF INTERESTS

P.A.G. is a member of Chem's advisory board.

REFERENCES

1. Gadsby, D.C. (2009). Ion channels versus ion pumps: the principal difference, in principle. Nat Rev Mol Cell Biol *10*, 344-352. https://doi.org/10.1038/nrm2668.
2. Dalemans, W., Barbry, P., Champigny, G., Jallat, S., Jallat, S., Dott, K., Dreyer, D., Crystal, R.G., Pavirani, A., Lecocq, J.-P., and Lazdunski, M. (1991). Altered chloride ion channel kinetics associated with the ΔF508 cystic fibrosis mutation. Nature *354*, 526-528. https://doi.org/10.1038/354526a0.
3. Gadsby, D.C., Vergani, P., and Csanady, L. (2006). The ABC protein turned chloride channel whose failure causes cystic fibrosis. Nature *440*, 477-483.
4. Gibson, R.L., Burns, J.L., and Ramsey, B.W. (2003). Pathophysiology and Management of Pulmonary Infections in Cystic Fibrosis. Am. J. Respir. Crit. Care Med. *168*, 918-951. https://doi.org/10.1164/rccm.200304-505SO.
5. Henderson, A.G., Ehre, C., Button, B., Abdullah, L.H., Cai, L.-H., Leigh, M.W., DeMaria, G.C., Matsui, H., Donaldson, S.H., and Davis, C.W. (2014). Cystic fibrosis airway secretions exhibit mucin hyperconcentration and increased osmotic pressure. J. Clin. Investig. *124*, 3047-3060. https://doi.org/10.1172/JCI73469.

6. Li, H., Valkenier, H., Thorne, A.G., Dias, C.M., Cooper, J.A., Kieffer, M., Busschaert, N., Gale, P.A., Sheppard, D.N., and Davis, A.P. (2019). Anion carriers as potential treatments for cystic fibrosis: transport in cystic fibrosis cells, and additivity to channel-targeting drugs. Chem. Sci. *10*, 9663-9672. 10.1039/C9SC04242C.
7. Wu, X., Judd, L.W., Howe, E.N.H., Withecombe, A.M., Soto-Cerrato, V., Li, H., Busschaert, N., Valkenier, H., Pérez-Tomás, R., Sheppard, D.N., et al. (2016). Nonprotonophoric Electrogenic Cl^- Transport Mediated by Valinomycin-like Carriers. Chem *1*, 127-146. https://doi.org/10.1016/j.chempr.2016.04.002.
8. Jowett, L.A., Howe, E.N.W., Soto-Cerrato, V., Van Rossom, W., Pérez-Tomás, R., and Gale, P.A. (2017). Indole-based perenosins as highly potent HCl transporters and potential anti-cancer agents. Sci. Rep. *7*, 9397. https://doi.org/10.1038/s41598-017-09645-9.
9. Wu, X., and Gale, P.A. (2016). Small-Molecule Uncoupling Protein Mimics: Synthetic Anion Receptors as Fatty Acid-Activated Proton Transporters. J. Am. Chem. Soc. *138*, 16508-16514. 10.1021/jacs.6b10615.
10. Wu, X., Small, J.R., Cataldo, A., Withecombe, A.M., Turner, P., and Gale, P.A. (2019). Voltage‐Switchable HCl Transport Enabled by Lipid Headgroup–Transporter Interactions. Angew. Chem. Int. Ed. *58*, 15142-15147. https://doi.org/10.1002/anie.201907466.
11. Busschaert, N., Park, S.-H., Baek, K.-H., Choi, Y.P., Park, J., Howe, E.N., Hiscock, J.R., Karagiannidis, L.E., Marques, I., and Félix, V. (2017). A synthetic ion transporter that disrupts autophagy and induces apoptosis by perturbing cellular chloride concentrations. Nat. Chem. *9*, 667–675. https://doi.org/10.1038/nchem.2706.
12. Ko, S.-K., Kim, S.K., Share, A., Lynch, V.M., Park, J., Namkung, W., Van Rossom, W., Busschaert, N., Gale, P.A., Sessler, J.L., and Shin, I. (2014). Synthetic ion transporters can induce apoptosis by facilitating chloride anion transport into cells. Nat. Chem. *6*, 885-892. https://doi.org/10.1038/nchem.2021.
13. Busschaert, N., Wenzel, M., Light, M.E., Iglesias-Hernández, P., Pérez-Tomás, R., and Gale, P.A. (2011). Structure–activity relationships in tripodal transmembrane anion transporters: the effect of fluorination. J. Am. Chem. Soc. *133*, 14136-14148. 10.1021/ja205884y.
14. Gilchrist, A.M., Chen, L., Wu, X., Lewis, W., Howe, E.N.W., Macreadie, L.K., and Gale, P.A. (2020). Tetrapodal Anion Transporters. Molecules *25*, 5179. https://doi.org/10.3390/molecules25215179.
15. Jowett, L.A., Howe, E.N.W., Wu, X., Busschaert, N., and Gale, P.A. (2018). New Insights into the Anion Transport Selectivity and Mechanism of Tren‐based Tris‐(thio)ureas. Chem. Eur. J. *24*, 10475-10487. https://doi.org/10.1002/chem.201801463.
16. Karagiannidis, L.E., Haynes, C.J.E., Holder, K.J., Kirby, I.L., Moore, S.J., Wells, N.J., and Gale, P.A. (2014). Highly effective yet simple transmembrane anion transporters based upon ortho-phenylenediamine bis-ureas. Chem. Commun. *50*, 12050-12053. 10.1039/C4CC05519E.
17. Gilchrist, A.M., Wu, X., Hawkins, B.A., Hibbs, D.E., and Gale, P.A. (2023). Fluorinated tetrapodal anion transporters. iScience *26*, 105988. https://doi.org/10.1016/j.isci.2023.105988.
18. Cao, R., Rossdeutcher, R.B., Zhong, Y., Shen, Y., Miller, D.P., Sobiech, T.A., Wu, X., Buitrago, L.S., Ramcharan, K., Gutay, M.I., et al. (2023). Aromatic pentaamide macrocycles bind anions with high affinity for transport across biomembranes. Nat. Chem. *15*, 1559-1568. 10.1038/s41557-023-01315-w.
19. Wu, X., Wang, P., Turner, P., Lewis, W., Catal, O., Thomas, D.S., and Gale, P.A. (2019). Tetraurea Macrocycles: Aggregation-Driven Binding of Chloride in Aqueous Solutions. Chem *5*, 1210-1222. 10.1016/j.chempr.2019.02.023.
20. Valkenier, H., Akrawi, O., Jurček, P., Sleziaková, K., Lízal, T., Bartik, K., and Šindelář, V. (2019). Fluorinated Bambusurils as Highly Effective and Selective Transmembrane Cl^-/HCO_3^- Antiporters. Chem *5*, 429-444. 10.1016/j.chempr.2018.11.008.
21. Mondal, A., Malla, J.A., Paithankar, H., Sharma, S., Chugh, J., and Talukdar, P. (2021). A Pyridyl-Linked Benzimidazolyl Tautomer Facilitates Prodigious H^+/Cl^- Symport through a Cooperative Protonation and Chloride Ion Recognition. Org. Lett. *23*, 6131-6136. https://doi.org/10.1021/acs.orglett.1c02235.
22. Liu, W., Oliver, A.G., and Smith, B.D. (2019). Stabilization and Extraction of Fluoride Anion Using a Tetralactam Receptor. J. Org. Chem. *84*, 4050-4057. 10.1021/acs.joc.9b00042.
23. Aquila, B., Ezhuthachan, J., Lyne, P., Pontz, T., and Zheng, X. (2007) Quinazoline Derivatives, Process for Their Preparation and Their Use as Anti-Cancer Agents. U. S. patent WO 2007/071963, patent application 12/097,965, 19/12/2006, and granted 22/12/2005.
24. Brown, A., Lang, T., Mullen, K.M., and Beer, P.D. (2017). Active metal template synthesis of a neutral indolocarbazole-containing [2]rotaxane host system for selective oxoanion recognition. Org. Biomol. Chem. *15*, 4587-4594. https://doi.org/10.1039/c7ob01040k.
25. Martí-Centelles, V., Burguete, M.I., and Luis, S.V. (2016). Macrocycle Synthesis by Chloride-Templated Amide Bond Formation. J. Org. Chem. *81*, 2143-2147. 10.1021/acs.joc.5b02676.
26. Mastalerz, M., Bhat, A., Elbert, S., Rominger, F., Zhang, W.-S., Schröder, R., and Dieckmann, M. (2019). Transformation of a [4+6] Salicylbisimine Cage to Chemically Robust Amide Cages. Angew. Chem. Int. Ed. *58*, 8819-8823. 10.1002/anie.201903631.
27. Ishikawa, N., Sugawara, S., and Watanabe, T. (1968). 5-Fluoroisophthalic Acid and its Derivatives. The Journal of the Society of Chemical Industry, Japan *71*, 519-522. https://doi.org/10.1246/nikkashi1898.71.4_519.
28. Costa, P.C.S., Barsottini, M.R.O., Vieira, M.L.L., Pires, B.A., Evangelista, J.S., Zeri, A.C.M., Nascimento, A.F.Z., Silva, J.S., Carazzolle, M.F., Pereira, G.A.G., et al. (2020). *N*-Phenylbenzamide derivatives as alternative oxidase inhibitors: Synthesis, molecular properties, ^{1}H-STD NMR, and QSAR. J. Mol. Struct. *1208*, 127903. https://doi.org/10.1016/j.molstruc.2020.127903.

29. Hibbert, D.B., and Thordarson, P. (2016). The death of the Job plot, transparency, open science and online tools, uncertainty estimation methods and other developments in supramolecular chemistry data analysis. Chem. Commun. 52, 12792-12805. 10.1039/C6CC03888C.
30. Thordarson, P. (2011). Determining association constants from titration experiments in supramolecular chemistry. Chem. Soc. Rev. *40*, 1305-1323. 10.1039/C0CS00062K.
31. Dias, C.M., Valkenier, H., and Davis, A.P. (2018). Anthracene Bisureas as Powerful and Accessible Anion Carriers. Chem. Eur. J. *24*, 6262-6268. 10.1002/chem.201800508.
32. Jowett, L.A., and Gale, P.A. (2019). Supramolecular methods: the chloride/nitrate transmembrane exchange assay. Supramol. Chem. *31*, 297-312. https://doi.org/10.1080/10610278.2019.1574017.
33. Clarke, H.J., Howe, E.N.W., Wu, X., Sommer, F., Yano, M., Light, M.E., Kubik, S., and Gale, P.A. (2016). Transmembrane Fluoride Transport: Direct Measurement and Selectivity Studies. J. Am. Chem. Soc. *138*, 16515-16522. 10.1021/jacs.6b10694.
34. Gilchrist, A.M., Wang, P., Carreira-Barral, I., Alonso-Carrillo, D., Wu, X., Quesada, R., and Gale, P.A. (2021). Supramolecular methods: the 8-hydroxypyrene-1,3,6-trisulfonic acid (HPTS) transport assay. Supramol. Chem. *33*, 1-20. https://doi.org/10.1080/10610278.2021.1999956.
35. Tetko, I.V., Gasteiger, J., Todeschini, R., Mauri, A., Livingstone, D., Ertl, P., Palyulin, V.A., Radchenko, E.V., Zefirov, N.S., Makarenko, A.S., et al. (2005). Virtual Computational Chemistry Laboratory – Design and Description. J. Comput. Aided Mol. Des. *19*, 453-463. https://doi.org/10.1007/s10822-005-8694-y.
36. VCCLAB (2005). Virtual Computational Chemistry Laboratory. https://www.vcclab.org.
37. Vieira, P., Miranda, M.Q., Marques, I., Carvalho, S., Chen, L.-J., Howe, E.N.W., Zhen, C., Leung, C.Y., Spooner, M.J., Morgado, B., et al. (2020). Development of a Library of Thiophene-Based Drug-Like Lego Molecules: Evaluation of Their Anion Binding, Transport Properties, and Cytotoxicity. Chem. Eur. J. *26*, 888-899. https://doi.org/10.1002/chem.201904255.
38. Valkenier, H., López Mora, N., Kros, A., and Davis, A.P. (2015). Visualization and Quantification of Transmembrane Ion Transport into Giant Unilamellar Vesicles. Angew. Chem. Int. Ed. *54*, 2137-2141. 10.1002/anie.201410200.
39. Wu, X., and Gale, P.A. (2021). Measuring anion transport selectivity: a cautionary tale. Chem. Commun. *57*, 3979-3982. 10.1039/D1CC01038G.
40. Steed, J.W., and Atwood, J.L. (2022). Supramolecular Chemistry, Third Edition (John Wiley & Sons Ltd).
41. Jing, L., Deplazes, E., Clegg, J.K., and Wu, X. (2024). A charge-neutral organic cage selectively binds strongly hydrated sulfate anions in water. Nat. Chem. *16,* 335-342. https://doi.org/10.1038/s41557-024-01457-5.
42. Butler, S.J. (2015). Quantitative determination of fluoride in pure water using luminescent europium complexes. Chem. Commun. *51*, 10879-10882. 10.1039/C5CC03428K.
43. Cataldo, A., Chvojka, M., Park, G., Šindelář, V., Gabbaï, F.P., Butler, S.J., and Valkenier, H. (2023). Transmembrane transport of fluoride studied by time-resolved emission spectroscopy. Chem Commun *59*, 4185-4188. https://doi.org/10.1039/d3cc00897e.
44. Park, G., Brock, D.J., Pellois, J.-P., and Gabbaï, F.P. (2019). Heavy Pnictogenium Cations as Transmembrane Anion Transporters in Vesicles and Erythrocytes. Chem *5*, 2215-2227. https://doi.org/10.1016/j.chempr.2019.06.013.
45. Park, G., and Gabbaï, F.P. (2020). Phosphonium Boranes for the Selective Transport of Fluoride Anions across Artificial Phospholipid Membranes. Angew. Chem. Int. Ed. *59*, 5298-5302. 10.1002/anie.201914958.
46. Yang, Y., Wu, X., Busschaert, N., Furuta, H., and Gale, P.A. (2017). Dissecting the chloride–nitrate anion transport assay. Chem Commun *53*, 9230-9233. https://doi.org/10.1039/C7CC04912A.

FIGURE AND SCHEME TITLES AND LEGENDS

Figure 1. The tetralactam anionophore library.

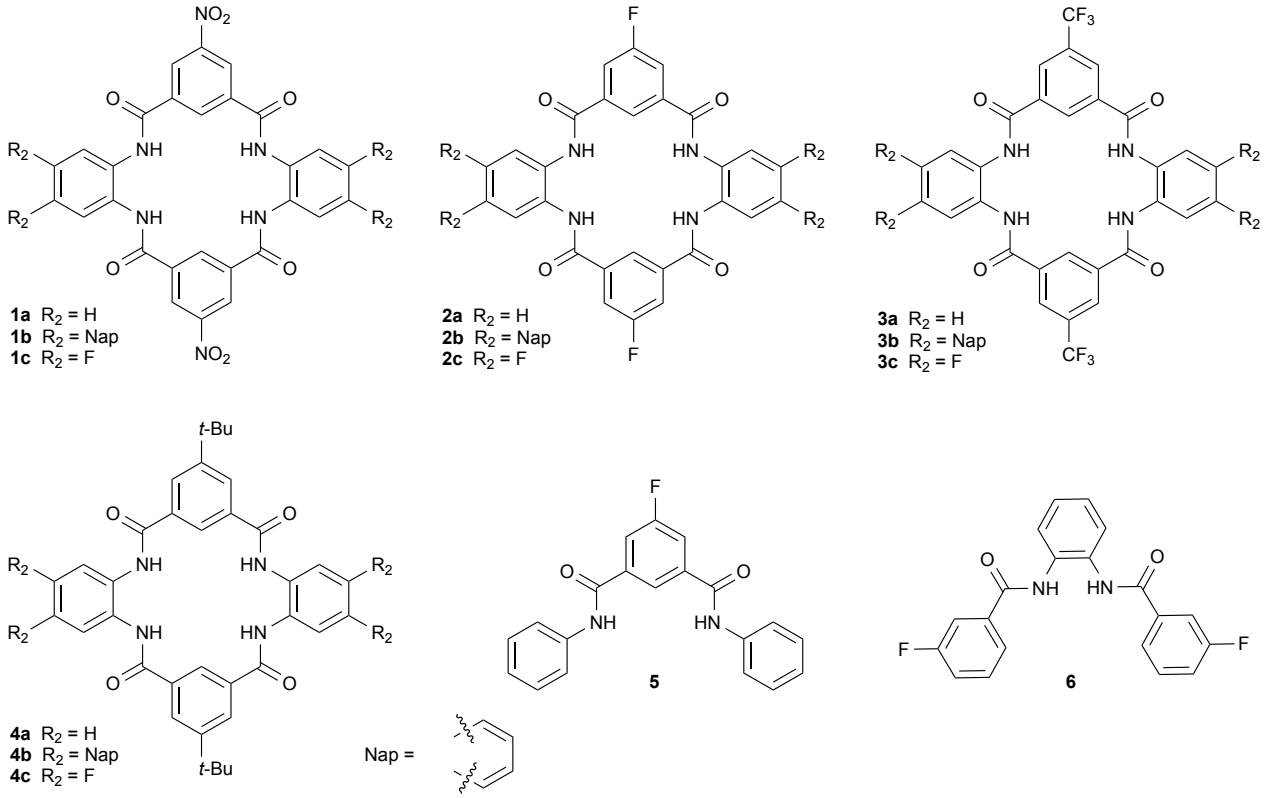

Tetralactams **1a—1c** contain the NO_2, **2a—2b** the F, and **3a—3c** the CF_3, and **4a—4c** the *t*-Bu functional group. Tetralactam **4a** has been previously reported by Smith and co-workers.[22]

Scheme 1. The two-step synthetic scheme of the tetralactam series (1a–4c) and the synthesis of the two previously reported isophthalamide (5) and benzamide (6) compounds.

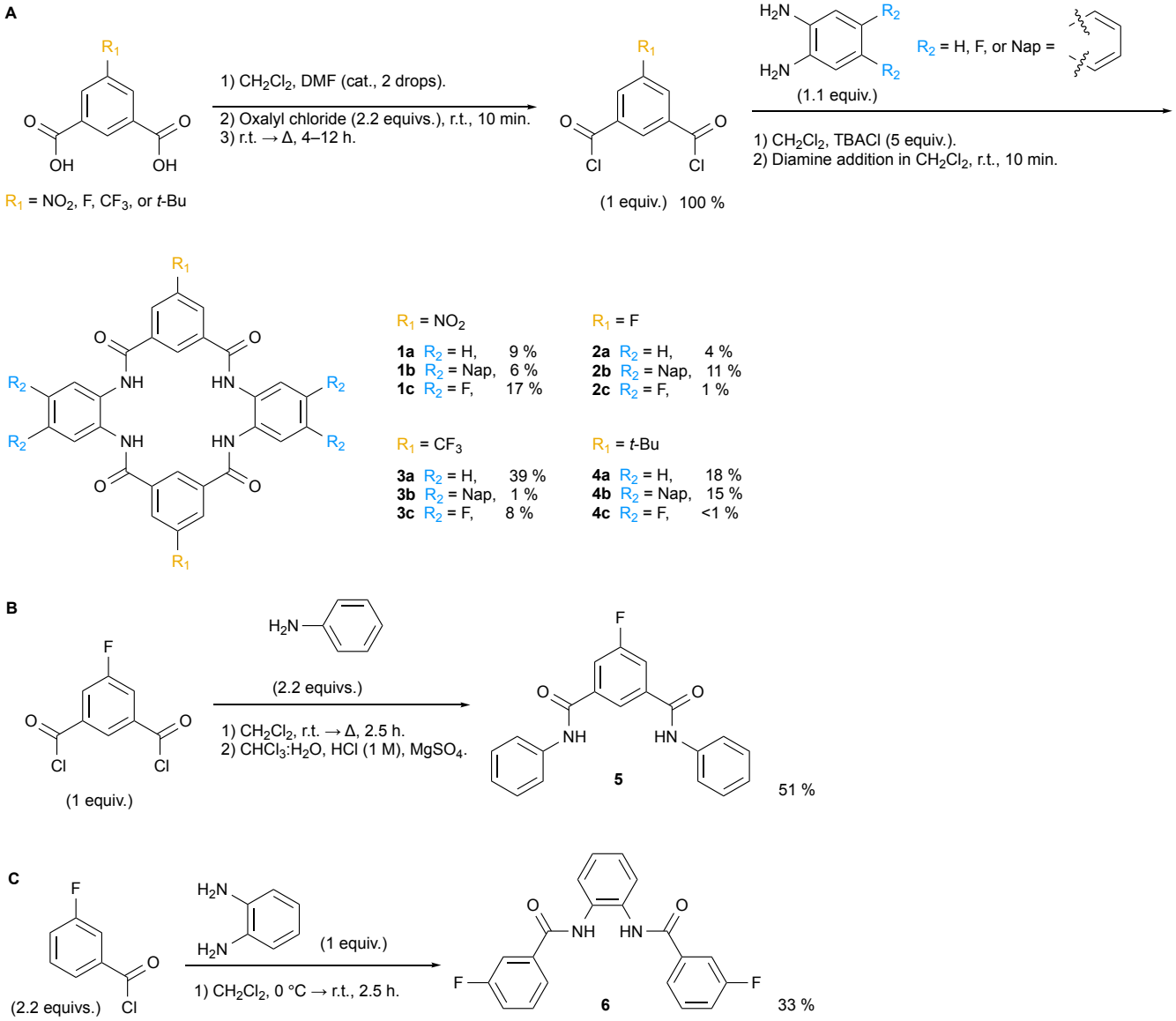

(A) The two-step synthetic method is used first to produce the desired isophthaloyl chloride intermediate and then the macrocyclic final products (**1a—4c**). R_1 (yellow) is representative of the substituent on the two isophthalamide units, and R_2 (blue) denotes the substituent of the two peripheral heterocyclic rings.
(B) The previously reported method by Ishikawa *et al.* to produce isophthalamide **5**.
(C) The previously reported method reported by Costa *et al.* to produce benzamide **6**.

Figure 2. The single crystal X-ray structures of the chloride complex of 2c·Cl⁻, the free host of receptor 3c, and the fluoride complex of 2a·F⁻.

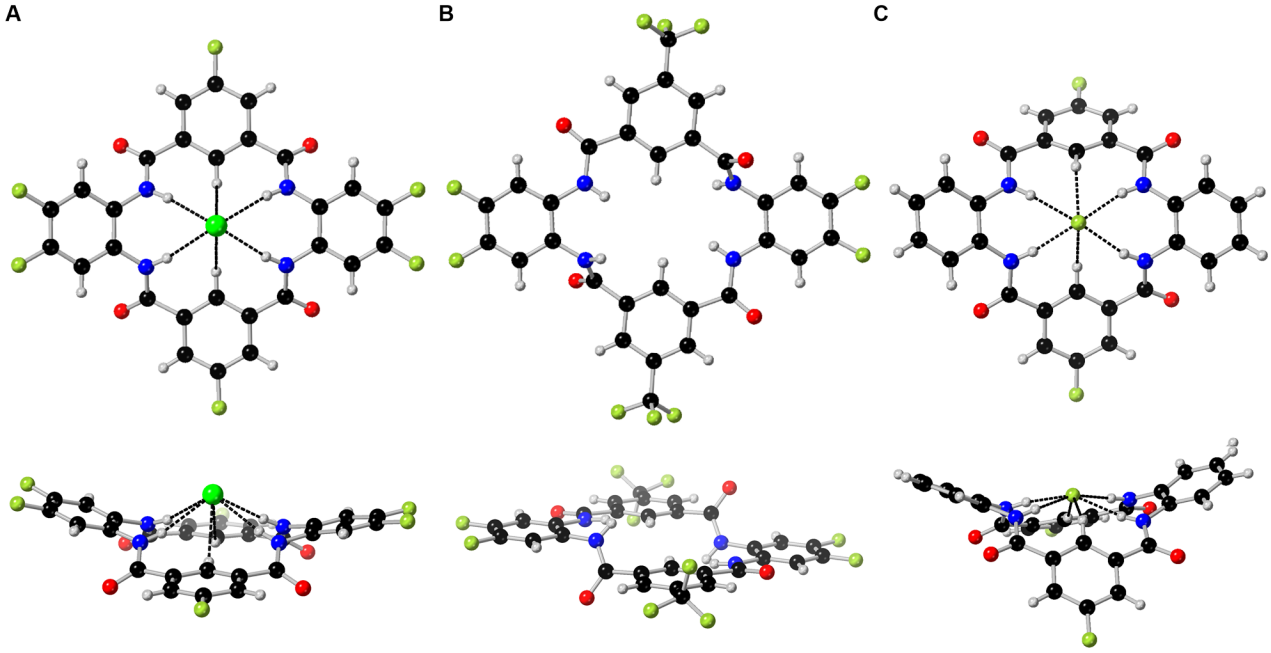

(A) The single crystal X-ray structure of receptor **2c** as the Cl^- complex (**2c·Cl⁻**) from the top and side.
(B) The single crystal X-ray structure of receptor **3c** as the free host structure from the top and side.
(C) The single crystal X-ray structure of receptor **2a** as the F^- complex (**2a·F⁻**) from the top and side. Broken black lines are used to represent hydrogen-bonding interactions. Hydrogen, carbon, nitrogen, oxygen, fluorine, and chlorine atoms are shown in grey, black, blue, red, lime green, and green, respectively. All solvents and TBA countercations in each structure have been removed for clarity.

Figure 3. A model system displaying the Cl^-/NO_3^- exchange assay conditions and experimental results from transporter 3c.

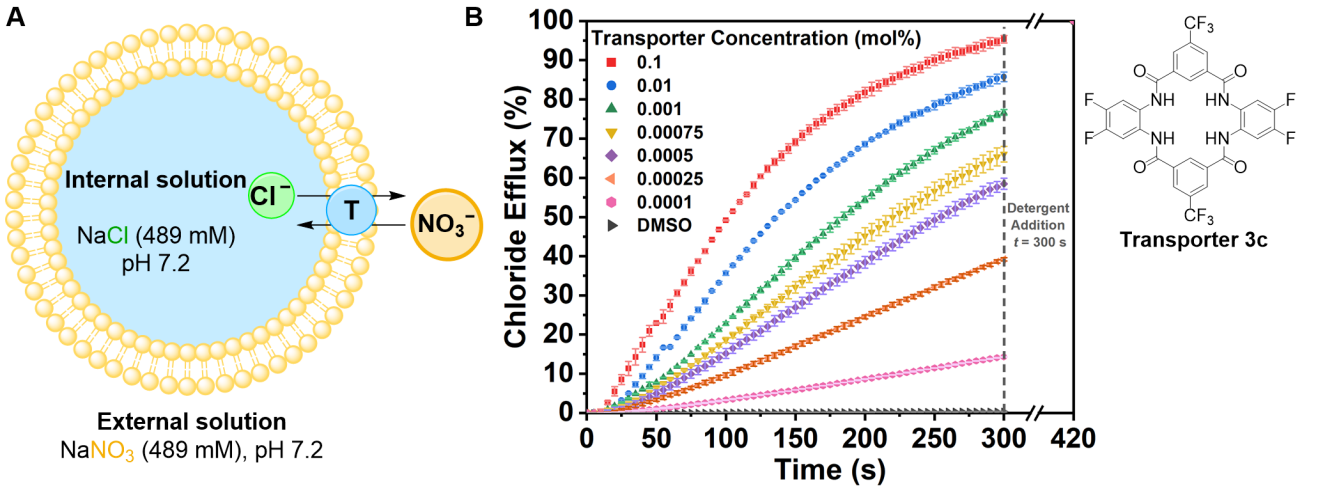

(A) A synthetic vesicle and the conditions of the Cl^-/NO_3^- ISE transport exchange assay, where a transporter (T, light blue) is added to perform Cl^- (green) transport, with the charged transport being balanced with the exchange of NO_3^- (orange).
(B) The normalised percentage Cl^- efflux elicited during the assay when transporter **3c** was tested at different concentrations in mol%, with respect to the lipid concentration.

Figure 4. Model synthetic systems displaying the conditions tested during the cationophore coupled transport assay.

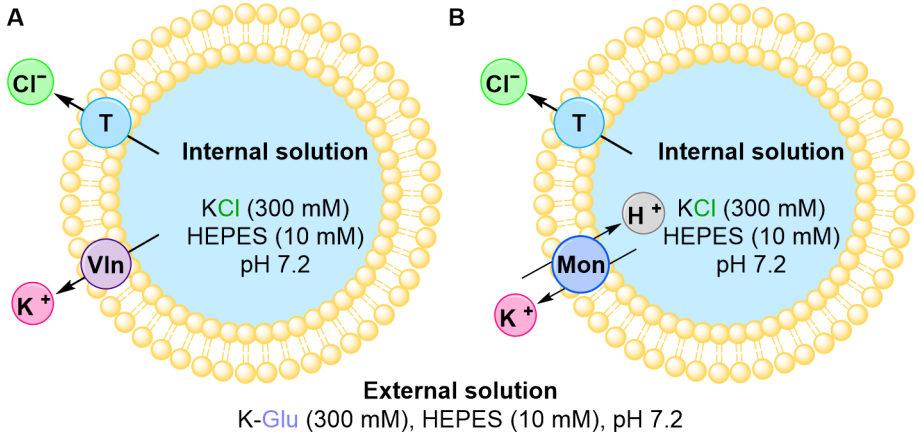

(A) The cationophore coupled assay conditions used to test the ability of the transporter to perform transport via an electrogenic Cl^- (or F^-) or uniport transport pathway using valinomycin (Vln, purple).
(B) The cationophore coupled assay conditions used to test the ability of a transporter to perform transport via an electroneutral H^+/Cl^- co-transport pathway using monensin (Mon, dark blue).

Figure 5. Three model synthetic vesicles showing the three main conditions tested during the HPTS transport selectivity assay and experimental results from transporter 2c.

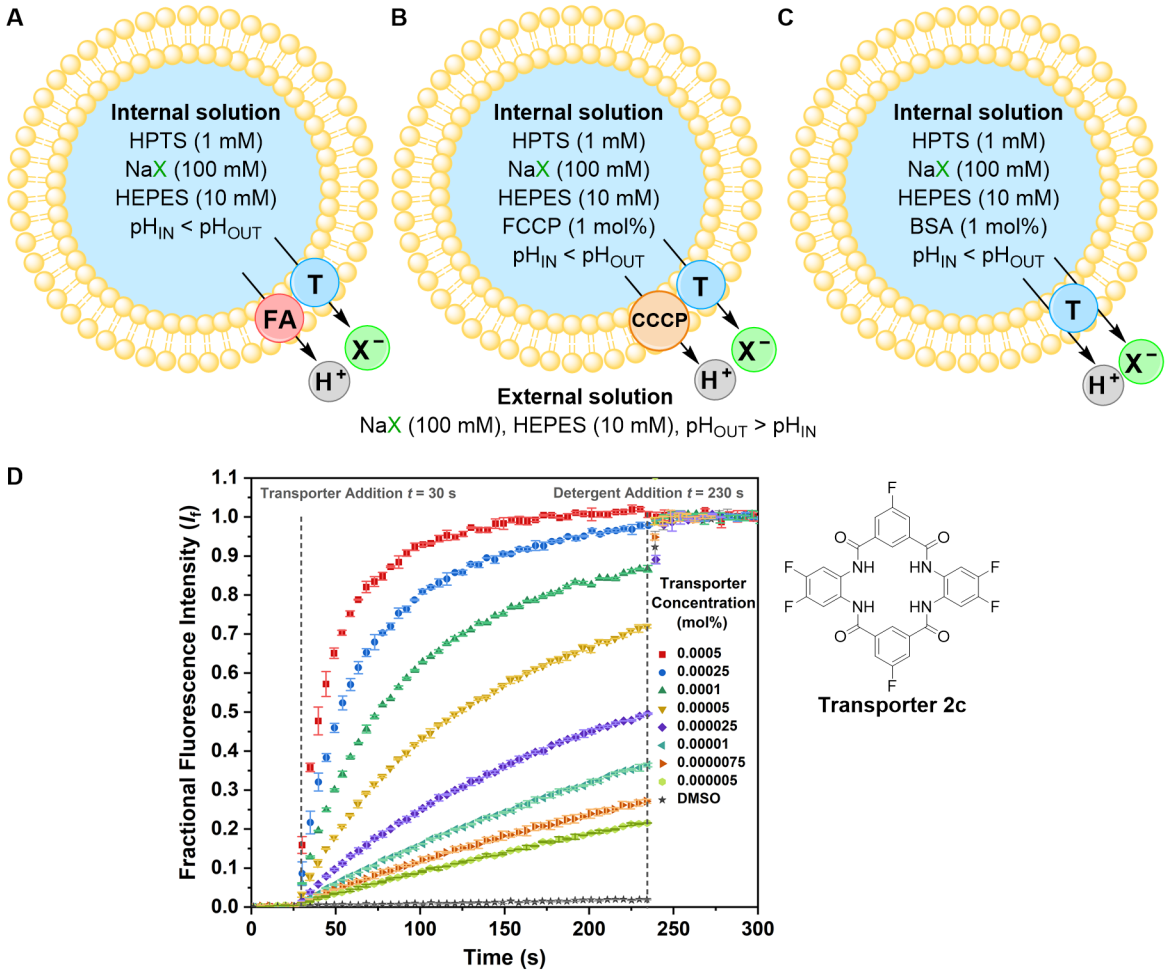

(A) The experimental conditions used to test the ability of a transporter to facilitate fatty acid (FA, red) assisted H^+/X^- (or OH^-/X^-, not shown) co-transport where the X^- is the anion of (X^-, green).
(B) The experimental conditions used to test a transporter for anion-selective transport (uniport) with vesicles treated with a weak acid protonophore (CCCP, orange).

(C) The experimental conditions used to test a transporter for non-selective co-transport via either H^+/Cl^- (symport) or OH^-/Cl^- (antiport) with vesicles treated with BSA.
(D) The experimental results of the Cl^- transport-induced change in fractional fluorescence intensity (I_f) recorded when transporter **2c** was added to a system of untreated vesicles at different concentrations (mol%) during the HPTS transport selectivity assay.

Figure 6. The normalised fluorescence intensity (I_f) graph of transporter 2c during the adjusted HPTS transport selectivity assay.

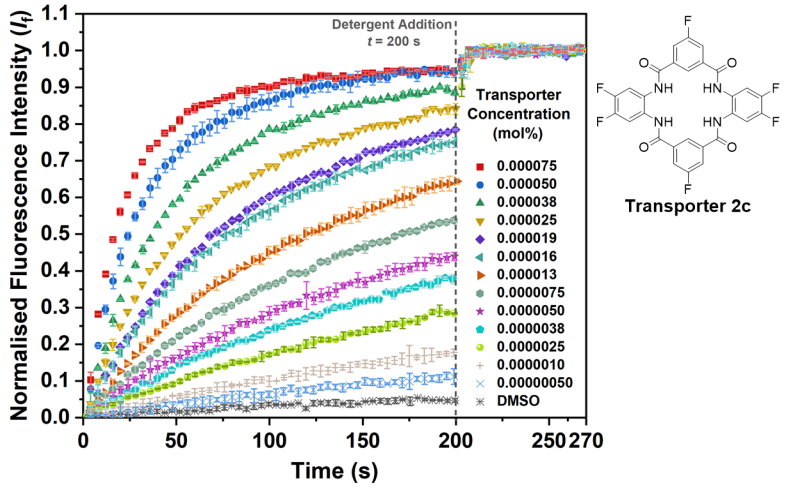

The normalised fluorescence intensity (I_f) graphed as a function of time when transporter **2c** was added to an adjusted HPTS transport selectivity assay system at varied concentrations. All error bars represent the standard deviation of two experiments.

Figure 7. The model synthetic system showing the conditions of the HPTS anion gradient assay and the experimental results of transporter 3c.

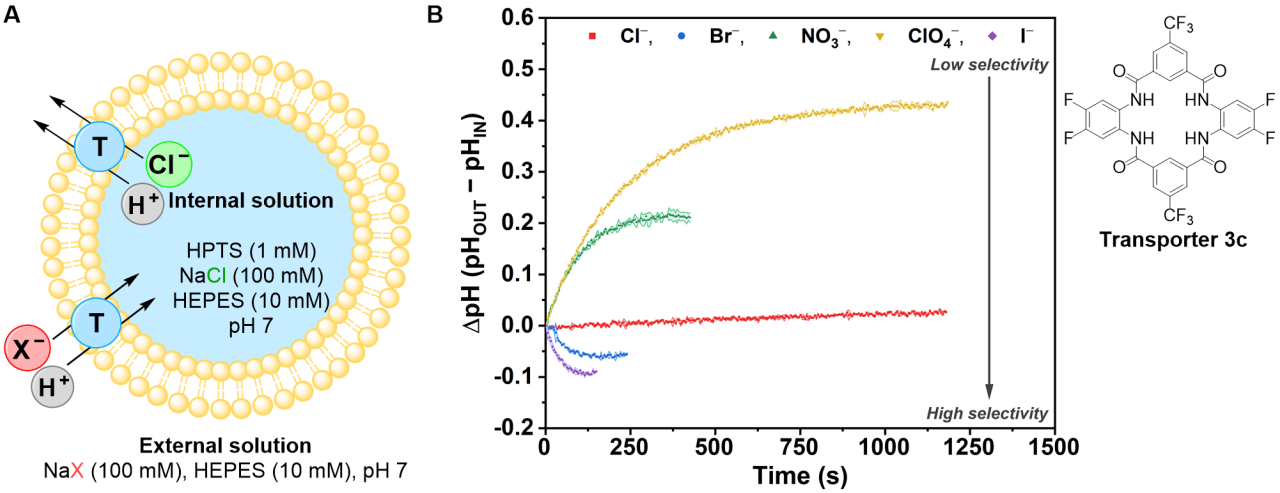

(A) A model synthetic vesicle displaying the conditions of the HPTS anion gradient transport selectivity assay where a rate of H^+/Cl^- efflux > H^+/X^- influx causes the basification of the vesicle interior and shows Cl^- > X^- selectivity. Also, acidification of the vesicle interior occurs when the rate of H^+/X^- influx > H^+/Cl^- efflux and shows X^- > Cl^- selectivity.
(B) The normalised anion transport selectivity of **3c** (0.000025 mM, 0.00005 mol%) was analysed using the HPTS anion gradient transport selectivity assay. Synthetic vesicles (200 nm) were suspended in different external solutions containing either Cl^- (red), Br^- (blue), NO_3^- (green), ClO_4^- (yellow), or I^- (purple).

Figure 8. A model vesicle system displaying the conditions used during the Eu(III) F^- transport assay and the experimental results when transporter 2c was tested.

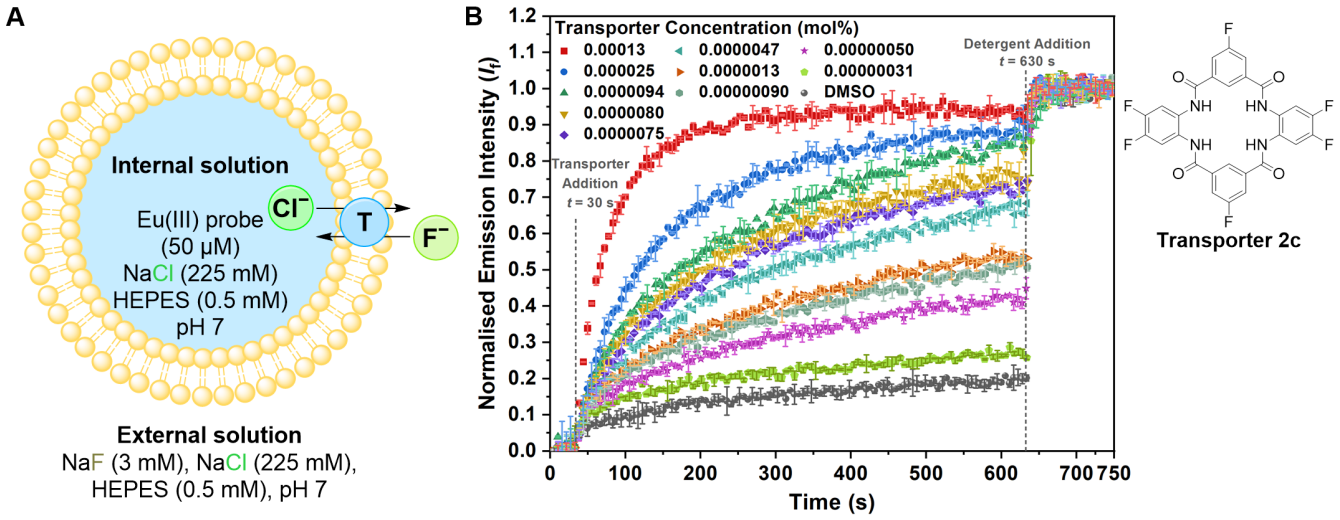

(A) A model vesicle system displaying the conditions used during the Eu(III) F^- transport assay where a base pulse containing NaF is added to form a F^- (lime green) concentration gradient where transporter-mediated F^- transport is detected using the luminescent Eu(III) probe.
(B) The normalised emission intensity (I_f) of the Eu(III) probe during the F^- transport assay after the addition of transporter **2c** as a DMSO solution at varied concentrations in mol%. All error bars represent the standard deviation between two repeated experiments.

TABLES AND TABLE TITLES AND LEGENDS

Table 1: The binding constants (K_a) of 1a–4c, 5 and 6 derived from fitting the data obtained from Cl^- titrations performed in DMSO-d_6/H_2O (0.5%).

Functional Group	Receptor	K_a (M^{-1}) [a]
NO_2	**1a**	1030
	1b	1530
	1c	2850
F	**2a**	445
	2b	459
	2c	1470
CF_3	**3a**	592
	3b	501
	3c	1620
t-Bu	**4a**	284
	4b	272
	4c	897
Acyclic [b]	**5**	16
	6	12

[a] See ESI for errors, and all studies were performed in DMSO-d_6/H_2O (0.5%) at 298 K. [b] Both receptors **5** and **6** are F-substituted acyclic compounds.

Table 2: The ISE Cl^-/NO_3^- exchange assay results and the EC_{50} values and Hill coefficients (*n*) derived from Hill analysis of the transport data produced by the tetralactams.

Functional Group	Transporter	EC_{50} (mol%) [a]	Hill Coefficient (*n*)
–F	**2a**	0.036	1.1
	2c	0.0012	1.1
$–CF_3$	**3a**	0.096	0.7
	3c	0.00043	1.4
–*t*-Bu	**4c**	0.015	1.2

[a] EC_{50} at 270 s, shown as receptor:lipid molar percentage.

Table 3: The k_{ini} rates of electrogenic and electroneutral transport and the electroneutral transport characters (ENC) of tetralactams 1a–4c.

Transporter	Initial Rate Constants (k_{ini},% s^{-1}) [a]			Electroneutral Transport Character (ENC) [b]
	Untreated Vesicles	Vln-treated Vesicles	Mon-treated Vesicles	
1a	0.033	0.084	0.27 [c]	3.2
1b	- [d]	- [d]	- [d]	- [e]
1c	0.059	0.070	0.40 [c]	5.7
2a	0.034	0.034	0.077	2.3
2b	0.025	0.024	0.056	2.3
2c	0.073	0.078	0.34 [c]	4.4
3a	0.055	0.085	0.65	7.6
3b	0.011	0.021	0.027	1.3
3c	0.056 [e]	0.068 [e]	0.30 [e]	4.4
4a	0.0051	0.025	0.021	0.84
4b	- [d]	- [d]	- [d]	-
4c	0.044	0.045	0.31 [c]	6.9

[a] The Cl^- efflux k_{ini} (% s^{-1}) rates facilitated by the tetralactams (0.05 mol%) in systems containing untreated vesicles or vesicles treated with either Vln or Mon (0.1 mol%). [b] The ENC factors of the tetralactams were calculated by dividing the k_{ini} rate achieved for the Mon-treated system by the k_{ini} rate achieved in the Vln-treated system. [c] Sigmoidal-shape kinetic curve observed likely due to slow partitioning of the transporters to the lipid bilayer membranes. The rates reported are the maximal rates obtained by differentiating the kinetic curves. [d] Accurate k_{ini} rates could not be obtained due to poor transporter solubility during the assay. [e] Due to high activity, the transporter loading of **3c** was decreased from 0.05 mol% to 0.0005 mol%.

Table 4: The EC_{50} (mol%) values of tetralactams 1a–4c obtained from the HPTS transport selectivity assay using untreated vesicles, CCCP-treated vesicles, BSA-treated vesicles, and the previously reported EC_{50} values for prodigiosin obtained using untreated vesicles.

Transporter	EC_{50} (mol%) [a]			CLogP [b]
	Untreated	CCCP	BSA	
1a	0.0089	0.015	0.11	2.85
1b	0.0059	0.0038	0.19	4.33
1c	0.000078	0.000067	0.00036	3.63
2a	0.041	0.22	0.39	3.47
2b	0.0030	0.0018	0.068	4.72
2c	0.000028	0.000030	0.00023	4.29
3a	0.0016	0.0019	0.00079	4.55
3b	0.0089	0.0048	0.0037	5.55
3c	0.000044	0.000060	0.000036	5.13
4a	0.46	0.17	0.53	4.86
4b	- [c]	- [c]	- [c]	5.84
4c	0.00081	0.00063	0.00036	5.51
Prodigiosin	0.000061 [d]	- [e]	- [e]	4.85

[a] All EC_{50} values are expressed in mol% with errors shown as the standard deviation of two separate experiments. [b] The CLogP values were calculated using the online ALOGPS 2.1 applet from VCCLAB.[35,36] [c] The transporter was too inactive and did not reach the required 50% Cl^- efflux, preventing an EC_{50} value from being calculated. [d] Previously reported by Gale and co-workers.[7] [e] Not determined.

Table 5: The EC_{50} (mol%) values and Hill coefficients (*n*) of 1a–4c obtained from Hill fitting the data obtained from the Eu(III) F^- transport assay.

Transporter	EC_{50} (mol%)	Hill Coefficient (*n*)
1a	0.00086	0.8
1b	0.0029	0.5
1c	0.0000088	1.6
2a	0.0035	1.1
2b	0.00042	0.6
2c	0.0000048	1.4
3a	0.00026	1.0
3b	0.00057	1.6
3c	0.000010	1.4
4a	0.050	0.8
4b	0.042	0.7
4c	0.000098	1.1